

## SMOS L1 Processor L1b Refactoring

**Code** : SO-TN-DME-L1PP-0169  
**Issue** : 1.3  
**Date** : 25/07/08

	<b>Name</b>	<b>Function</b>	<b>Signature</b>
<b>Prepared by</b>	N. Catarino	Project Engineer	
<b>Checked by</b>	J. Freitas	Quality A. Manager	
<b>Approved by</b>	J. Barbosa	Project Manager	

DEIMOS Engenharia  
Av. D. João II, Lote 1.17, Torre Zen, 10º,  
1998-023 Lisboa, PORTUGAL  
Tel: +351 21 893 3013  
Fax: +351 21 896 9099  
E-mail: <mailto:deimos@deimos.com.pt>

© DEIMOS Engenharia 2008

All Rights Reserved. No part of this document may be reproduced, stored in a retrieval system, or transmitted, in any form or by any means, electronic, mechanical, photocopying, recording or otherwise, without the prior written permission of DEIMOS Engenharia

This page intentionally left blank

## Document Information

Contract Data	Classification
Contract Number: DE04/B-434/P	Internal <input checked="" type="checkbox"/>
Contract Issuer: EADS CASA Espacio	Public <input type="checkbox"/>
	Industry <input type="checkbox"/>
	Confidential <input type="checkbox"/>

Internal Distribution		
Name	Unit	Copies

External Distribution		
Name	Organisation	Copies
Michele Zundo	ESA	1
Josep Closa	EADS CASA Espacio	4

Archiving	
Word Processor:	MS Word 2000
File Name:	SO-TN-DME-L1PP-0169-L1b-Refactoring.doc
Archive Code:	

## Document Status Log

Issue	Change description	Date	Approved
1.0	First draft	2008-01-20	
1.1	Updated after comments from MMN	2008-02-22	
1.2	Internal delivery to ESTEC for review before PM#1	2008-04-23	
1.3	First official delivery	2008-07-25	

## Table of Contents

<b>1. Introduction .....</b>	<b>6</b>
<b>1.1. Purpose and Scope .....</b>	<b>6</b>
<b>1.2. Applicable and Reference Documents.....</b>	<b>6</b>
1.2.1. Applicable Documents .....	6
1.2.2. Reference Documents .....	7
<b>1.3. Statement of Work.....</b>	<b>8</b>
1.3.1. Architecture Re-Design.....	8
1.3.2. Implementation of Re-Designed L1b.....	9
1.3.3. Study of Scene Dependent Bias and L1b Performance.....	9
<b>2. Image Reconstruction in the SMOS L1 Processor .....</b>	<b>10</b>
<b>2.1. High Level Description .....</b>	<b>10</b>
<b>2.2. Image Reconstruction Module.....</b>	<b>12</b>
2.2.1. Zero Baselines Visibilities Processing .....	16
<b>2.3. Main Loop .....</b>	<b>18</b>
2.3.1. Foreign Sources Computation Sub-module Details .....	21
2.3.2. Error Mitigation Sub-module .....	39
<b>2.4. L1c Implications.....</b>	<b>41</b>
<b>3. Memory Management Design Options.....</b>	<b>43</b>
<b>4. L1b Flags.....</b>	<b>45</b>
<b>5. Breakpoints and Logs .....</b>	<b>47</b>
<b>6. Internal Notes .....</b>	<b>50</b>

## List of Figures

Figure 1: Context Diagram for L1a to L1b processing.....	10
Figure 2: First detailed Data Flow Diagram for L1a to L1b processing.....	12
Figure 3: Image Processing Module, including Foreign Sources Correction and Error Mitigation.....	15
Figure 4: Simplified Data Flow Diagram of the processing of the NIR (zero) baselines.....	16
Figure 5: Simplified Flowchart of the processing of the zero baselines Visibilities. ....	17
Figure 6: Simplified Flowchart of the processing of the nominal (i.e. non-zero) baselines Visibilities. ....	17
Figure 7: Detailed Data Flow for the loop in the number of scenes.....	21
Figure 8: Foreign Sources Calculation Sub-module.....	23
Figure 9: Contour of the earth computed using the xp_target_altitude CFI function.....	24
Figure 10: Error Mitigation sub-module. ....	40
Figure 11: L1c DFD .....	42

## List of Tables

Table 1: Applicable Documents .....	6
Table 2: Reference Documents.....	8
Table 3: Memory footprint for the largest data structures needed in L1b.....	43
Table 4: L1b processing flags.....	46
Table 5: L1b breakpoints and validation status.....	49

## 1. INTRODUCTION

### 1.1. Purpose and Scope

This document describes the strategy for the restructuring of the L1b module of the L1PP. The goal is to be used as an informal working document, where the implementation analysis is detailed for further discussion.

### 1.2. Applicable and Reference Documents

#### 1.2.1. Applicable Documents

Ref.	Code	Title	Issue
AD.1	SO-SOW-CASA-PLM-0385	Level 1 Processor Prototype Development Phase 3 and Support Activities. Statement of Work	<b>01</b>
AD.2	SO-RS-ESA-PLM-0003	SMOS System Requirements Document	<b>3.0</b>
AD.3	SO-IS-DME-L1PP-0014	SMOS L1 Processor Input Output Data Definition	<b>2.3</b>
AD.4	SO-IS-DME-L1PP-0002	SMOS L1 Product Format Specification	<b>2.3</b>
AD.5	SO-IS-DME-L1PP-0003	SMOS L1 Auxiliary Data Format Specification	<b>2.3</b>
AD.6	SO-TN-UPC-PLM-01	IN-ORBIT CALIBRATION PLAN	<b>3.3</b>
AD.7	SO-TN-UPC-PLM-0019	SMOS In Orbit Calibration Plan Phase C-D	<b>1.5</b>
AD.8	ECSS-E-40B	ECSS E-40 Software Engineering Standards	
AD.9	SO-DS-DME-L1PP-0011	SMOS L1 Algorithm Theoretical Baseline	<b>2.9</b>
AD.10	SO-DS-DME-L1PP-0006	SMOS L1 System Concept	<b>2.8</b>
AD.11	SO-DS-DME-L1PP-0012	SMOS L1 Processor Prototype Architecture	<b>1.3</b>
AD.12	SPS-TN-GMV-PL-0003	SMOS End-to-End Performance Simulator (SEPS) Architectural and Detailed Design Document	<b>5.0</b>
AD.13	SO-TN-UPC-PLM-0010	Distributed Amplitude Calibration by the Two-Level Approach	<b>1.0</b>

**Table 1: Applicable Documents**

## 1.2.2. Reference Documents

Ref.	Code/Author	Title	Issue
RD.1	SPA-CAS-20200-TNO-001	System Performance Modelling	1.2
RD.2	R. Butora, M. Martín-Neira, A.L. Rivada,	<i>“Fringe-Washing Function Calibration in Aperture Synthesis Microwave Radiometry”</i> , Radio Science Vol. 38 No. 2, p. 1032	2003
RD.4	SO-DS-DME-L1PP-0007	SMOS L0 to L1a Detailed Processing Model	2.5
RD.5	SO-TN-DME-L1PP-0024	SMOS L1 Full Polarisation Data Processing	1.6
RD.6	SO-TS-HUT-NIR-0005	NIR Calibration and Characterisation Plan	05E
RD.7	SO-TN-YLIN-NIR-0006	SMOS Phase C/D NIR Subsystem, NIR Technical Description	05A
RD.8	SO-TN-UPC-PLM-0020	Technical Note on the Calibration by Moon Pointing	1.1
RD.9	E. Anterrieu	<i>“A resolving matrix approach to synthetic aperture imaging radiometer”</i> , IEEE Trans. Geosc. and Remote Sensing, Vol. 42, No.8, <i>“Stabilised Reconstruction algorithm presentation”</i> , ESTEC	2004
RD.10	E. Anterrieu	<i>“Hexagonal xi-eta grid”</i> , response email to DME xi-eta grid question with attached matlab code	13th May 2005
RD.11	A. Camps et al	<i>“Impact and Compensation of Diffuse Sun Scattering in 2D Aperture Synthesis Radiometers Imagery”</i> , IGARSS	2005
RD.12	A. Camps et al	<i>“Sun Effects in 2-D Aperture Synthesis Radiometry Imaging and their Cancellation”</i> , IEEE transactions on geoscience and remote sensing Vol. 42, No. 6	June 2004
RD.13	A. Camps et al	<i>“The processing of hexagonally sampled signals with standard rectangular techniques: application to 2-D large aperture synthesis interferometric radiometers”</i> , IEEE Trans. geosc. and remote sensing, Vol. 35, No.1, pp. 183-190.	Jan. 1997
RD.14	A. Camps	<i>“Application of Interferometric Radiometry to Earth Observation”</i> , PhD Dissertation, Universitat Politècnica de Catalunya	November 1996
RD.15	M. Goodberlet and J. Miller	<i>“NPOESS-Sea Surface Salinity”</i> , Final Report, NOAA Contract #43AANE704017	December

Ref.	Code/Author	Title	Issue
			1997
RD.16	SMOSP3-UPC-TN-0002 v 1.0	“Sun Self-estimation Algorithm” <sup>1</sup>	May 2007
RD.17	SMOSP3-UPC-TN-0002 v 1.0	“Sun Self-estimation Algorithm: Simulation Results”	July 2007

**Table 2: Reference Documents**

## 1.3. Statement of Work

The following is the technical proposal text taken from the DME document SMOSL1-DME-PRO-011<sup>2</sup>:

### 1.3.1. Architecture Re-Design

The L1b processing module has been heavily upgraded since its initial design in Phase 2. The Flat Target Transformation is an add-on module that can be only selected in opposition to Earth/Sky Removal. The Foreign Sources removal code can also be optimised with the respect to the current implementation, although this has been postponed many times in favour of new functionalities and stability of L1PP.

Recently a new approach has been proposed by ESA to integrate FTT and Earth/Sky Removal in a single unified method of pre-processing the images before reconstruction with the J+ method. The approach currently under study is summarised as:

- FTT is applied first of all to L1a calibrated visibilities in order to produce differential visibilities. The FTT scaling factor is composed by an average of NIR H and V pol measurements.
- The FTT differential has to be corrected AFTER reconstruction, by adding back the non-uniformity of the FTT scene, and the constant reference ( $T_{ref} = \langle T_B \rangle$ ) temperatures. This is currently done at the end of L1b processing still in the Fourier domain.
- Sun/Moon/SunGlint/Backlobe effects are removed from the differential visibilities. These effects will be removed permanently and nothing will be added back to the image;
- Gibbs effects of type 1 are removed by subtracting the Sky in the Unit Circle. The Sky to be subtracted has to be modified as the L1PP is currently working with differential visibilities, so the temperature to remove is  $T_{sky} - T_{nir}$  (where  $T_{nir}$  is the averaged NIR BT used in the FTT scaling factor);

<sup>1</sup> Document available at the L1PP project webpage: [http://www.smos.com.pt/project\\_results.html](http://www.smos.com.pt/project_results.html)

<sup>2</sup> “Proposal to EADS - CASA Espacio for the SMOS Level 1 Processor Prototype Development Phase 4 and Support Activities (In response to SoW SO-SOW-CASA-PLM-1317)”, issue 1.0, of 20/12/07

- Gibbs effects of type 1 have to be corrected AFTER reconstruction, by adding back the  $T_{nir}$  which was subtracted. This addition has to be performed during L1c processing as a constant offset, in the same way as it is done for the constant Earth. The Sky is not added back, as the purpose of the removal is to extend the FOV.  $T_{nir}$  has to be added back only where there is a Sky alias;
- Gibbs effects of type 2 are removed by subtracting two constant BT magnitudes, one for land and another one for sea. The BT magnitudes shall be contained initially in the configuration file. A land-sea mask will be used to divide the Earth within the unit circle into 128x128 points of land and sea. These points will be multiplied by the G matrix in order to compute the Gibbs#2 visibilities. These visibilities shall also be subtracted from the FTT differential visibilities available.
- Gibbs effects of type 2 have to be corrected AFTER reconstruction, by adding back the land/sea BT that was subtracted. There are several approaches for this, and a baseline is not clear:
  - DGG land/sea masked is used: this means that interpolation is needed during L1b processing to transform the DGG into each snapshot 128x128 unit circle. However, L1c processing is clean as each point knows immediately which quantity (land or sea) has to be added back;
  - Common land/sea model is used (USGS, other): interpolation is needed now in L1b and L1c processing, but it should be simpler to do as the models already incorporate that feature. Has the benefit that the same model is used in L1b and L1c;

During the course of this activity, a full re-design of the L1b processing module will be made around the needs of the new integrated approach and taking advantage of this fact to optimise the Foreign Sources removal methods. A design document shall be written and will be presented to ESA/CASA for discussion before the implementation is started.

### **1.3.2. Implementation of Re-Designed L1b**

In this activity, the L1b processing module will be essentially re-coded to conform to the new design. Whenever possible, the old methods and functionalities will be retained for comparison and backward compatibility needs. Also in the scope of this activity is the full validation of the method against the results obtained in Phase 3.

### **1.3.3. Study of Scene Dependent Bias and L1b Performance**

A study will be made on the relative performance gains of the new integrated approach for L1b processing. Care will be taken to analyse separately the removal of Gibbs effects of type 1 and type 2 and their influence on the Scene Dependent Bias.

## 2. IMAGE RECONSTRUCTION IN THE SMOS L1 PROCESSOR

The image reconstruction is the most important part of the SMOS processor. It converts Calibrated Visibilities into Brightness Temperature Fourier components (see Figure 1). These Fourier components represent the reconstructed image in the Frequency domain, and can be used to obtain the Brightness Temperature values anywhere in the spatial domain. This reconstruction step is not reversible, once the Brightness Temperatures Fourier components are calculated, meaning that if the algorithms evolve in some way, it shall be necessary to re-process the L1a data to obtain the new L1b data.

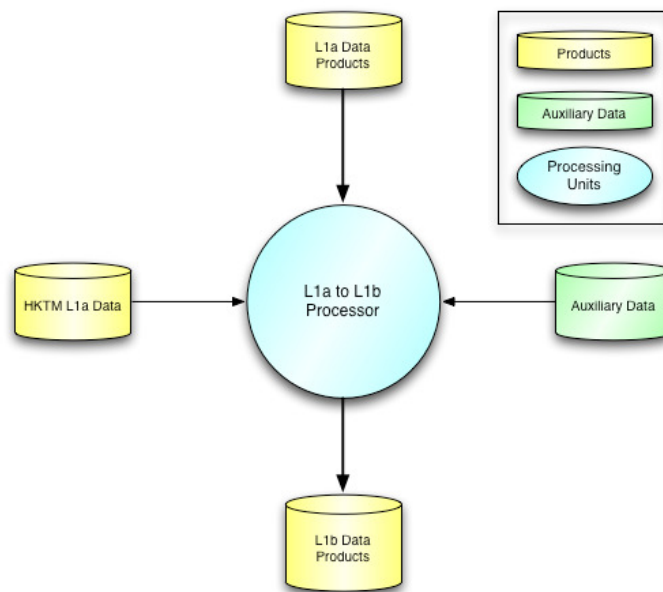


**Figure 1: Context Diagram for L1a to L1b processing.**

At this high level there is no change to the L1b processor wrt the [DPM L1b v2.4](#).

### 2.1. High Level Description

The main functionality of the L1a to L1b Processor is to do reconstruction of the L1a Calibrated Visibilities. The main module is therefore the *Image Reconstruction Module* (including Foreign Sources Correction and Error Mitigation), which transforms the calibrated visibilities into Brightness Temperature Fourier components. The output of this transformation are the L1b products that are consolidated in the same way as the L1a, containing Brightness Temperature Fourier components arranged in a time-ordered way according to the integration time. This time ordering has the effect that a given pixel may be contained in different snapshots, depending on the incidence angle with which the image was taken. The output to be passed to the L1c shall be the Fourier components of the reconstructed BT scene.

In addition to the main Image Reconstruction Module, two other accessory modules are also implemented in the L1PP: the *G/J<sup>+</sup>-matrices Generator Module* and the *Flat Target Generator Module* (see the DFD in Figure 2).

The G and  $J^+$ -matrices Generator Module is responsible for the computation of the best approximation to the System Response Function (G-matrix) and to invert it (in the  $J^+$ -matrix) for use with the L1a measurement products. Any external calibration or validation of the System Response Model shall be communicated to this module, so that it is able to update the modelling. This System Response Function, for example, shall be recomputed with any new calibration of the Fringe Washing Function (FWF), as it forms an inherent part of it

The Flat Target Generator Module is responsible for generating an Auxiliary Data File for use in the Flat Target Transformation module. This data file is generated from External Target data, and contains information on a flat sky target, which is used by the Image Reconstruction Module to reduce the errors due to the Antenna Patterns (see Section 2.3.2.1).

The L1PP being a data driven Processor, the selection of which module are invoked is determined by the input data in the following way (this is also illustrated in Figure 2):

- If L1a Science Data is present, then it is processed by the Image Reconstruction Module;
- If External Target data is present instead, then the Flat Target Auxiliary Data File (ADF) is generated and then the Image Reconstruction Module is also invoked<sup>3</sup>;
- If new Fringe Washing Function data is present, then new G and  $J^+$ -matrices are generated.

---

<sup>3</sup> The image processing of the External Target data is similar to the processing of Science data, except that: a) Sun Glint correction is not performed; b) L1c processing is turned off since there is no geolocation data; c) Sky removal depends on a new flag specific to External Target processing (see *Table 4*).

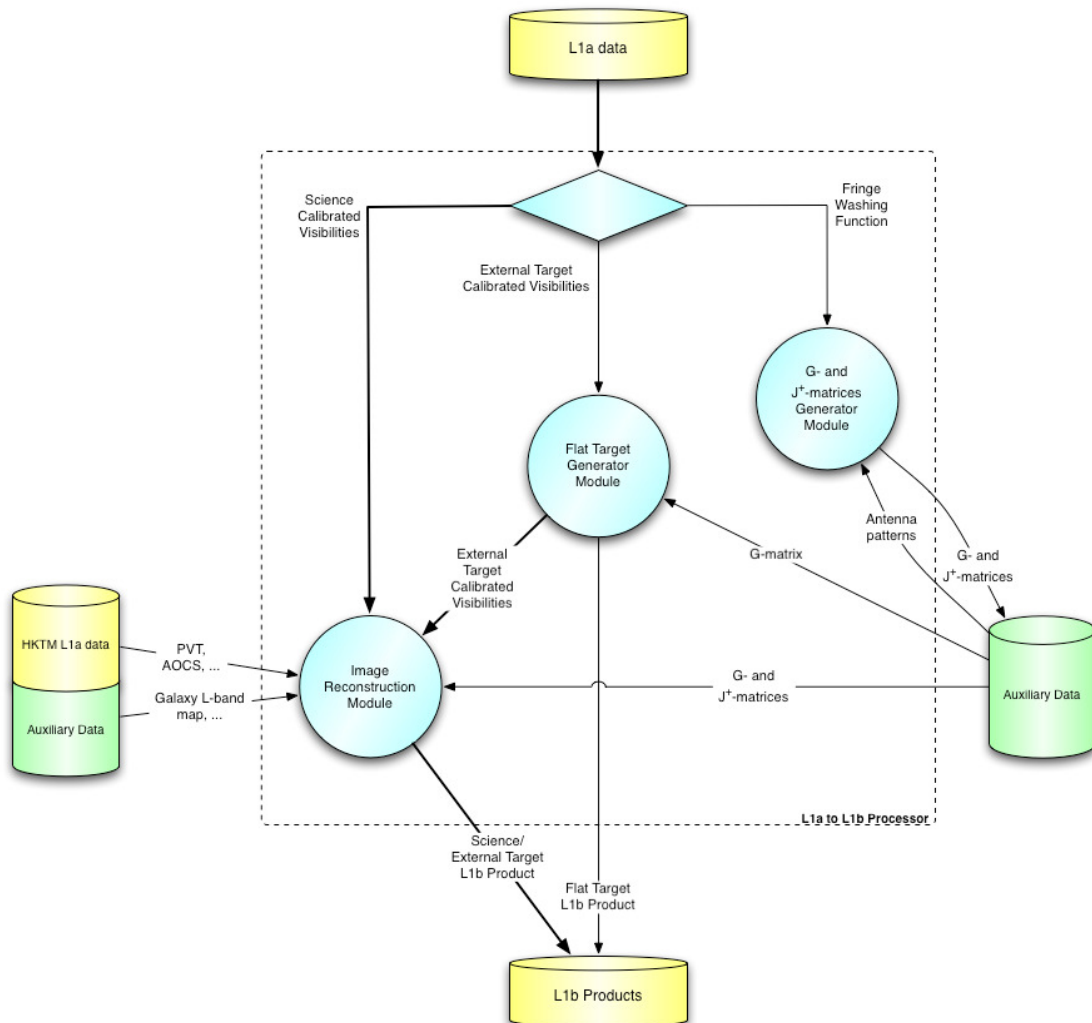


**Figure 2: First detailed Data Flow Diagram for L1a to L1b processing.**

Of the three modules above, only the Image Reconstruction Module suffered changes wrt the current baseline, so only this module will be detailed in this document. Detailed descriptions of the G and J<sup>+</sup>-matrices Generator and Flat Target Generator Modules can be found in the [DPM L1b v2.4](#).

## 2.2. Image Reconstruction Module

The Image Reconstruction (IR) Module is responsible for loading the L1a data, performing the appropriate transformations on the data in order to remove unwanted sources of signal and to reduce reconstruction errors, and finally for the reconstruction of the data and product writing. These processing steps of the IR Module are organized into eight processing units (nine when in External Target mode), of which two are major ones (semi-independent sub-modules) and six minor ones (see *Figure 3*). For the whole L1b Processor there is an orchestrator which deals with the computational sequence, calling each unit according to the diagram in *Figure 3*.

The distinction between minor and major units is twofold, since the major units are where the algorithms are much more complex, but also they deserve a distinct processing approach: the major

units (Foreign Sources Computation and Error Mitigation) are processed scene by scene in a loop for the total number of scenes, whereas the in the minor units all scenes are processed simultaneously. This is done to improve code optimisation, as detailed in Section 3.

The **minor processing units** should be included in the main L1b source file, since they are not too complex:

1+2) **Data Loading and Preprocessing Units**: these processing units consist in the loading of the required data and conversion from the Aux and/or L1a structure to L1b format, including the calculation of the land-sea pixels in the  $(\xi, \eta)$ -grid and other preparatory tasks. These are simple tasks, although the conversion of the Calibrated Visibilities to L1b format has some increased complexity in the full-pol case.

After these two units the processing goes into the main loop in the number of scenes, where most of the image correction computations are performed. Since these are more complex task they will be detailed separately.

The last four minor processing units are simultaneously applied to all scenes (and are therefore outside and after the loop in *Figure 3*):

- 5) **G-matrix Multiplication**: here the Loop Temperature Contrast Vectors (Sky plus Land, Sea and Sun Glint) computed in the Foreign Sources Computation and Error Mitigation Modules (see below) are multiplied by the G-matrix to determine the corresponding Loop Transformed Visibilities. This is a computationally heavy task since the complete G-matrix alone is quite large (see also Section 3).
- 6) **Final Subtraction of Calculated Visibilities**: this is the simplest activity, which the subtraction of the output of the G-matrix Operations unit, the Loop Transformed Visibilities, from the Calibrated Visibilities.
- 7) **Image Reconstruction**: this is the main reconstruction unit, which converts the Calibrated Visibilities into Brightness Temperatures' Fourier Components,  $C_{B,r}^q(\mathbf{u})$ , by multiplying the Visibilities by the  $J^+$ -matrix. If Ideal Reconstruction mode is selected, however, the reconstruction is performed through an FFT instead of the  $J^+$ -matrix multiplication.
- 8) **Adding the Reference Temperature back**: adding the Reference Temperature,  $T_{Ref}$ , is only performed in the L1b Module when processing External Target data, since it is otherwise a task performed in L1c (see Section 2.4). Since the L1c Module cannot be executed with data acquired in External Target mode, this task is instead performed in the L1b Module;
- 9) **Writing of L1b Products**.

As for the **major sub-processing units or sub-modules**, these are the following:

- 3) **Foreign Sources Correction Module**: this sub-module calculates and removes the unwanted contributions from the Visibilities. It determines the Sky, Direct Sun, Direct Moon, Sun Glint and Backlobes contributions and removes them from the Calibrated Visibilities - this last contribution, the Backlobes, are removed only for the zero baseline (NIRs). Although strictly part of the Error Mitigation Module<sup>4</sup>, a Sea Temperature and a "One Kelvin Land Temperature Vector" are also calculated here (see sub-section 2.3.1 for details). These are later on passed on to the Error

---

<sup>4</sup> The conceptual distinction between what should be considered as part of the Foreign Sources Removal or of the Error Mitigation is, in broad terms, that the FS contributions (Sun, Moon, etc.) are not added back, whereas the quantities calculated by Error Mitigation Module (Land, Sea and Reference Temperature) are removed only to decrease the reconstruction errors, and should be re-added later on, e.g. in the L1b to L1c processor.

Mitigation Module for the estimation of the Land temperature. Finally, auxiliary data is also passed on to the L1c processor, in particular the Sun and Moon positions and magnitudes.

- 4) Error Mitigation Module: this sub-module performs the correction of the Corbella term for the System Response Function by setting a global reference temperature<sup>5</sup>, and also performs the calculations needed for the Gibbs removal, namely of the Land and Sea temperature vectors. The setting of a global Reference Temperature is done by removing the contribution of a flat (i.e. constant) scene at a given temperature,  $T_{\text{Ref}}$ , from the Calibrated Visibilities. This constant scene should be obtained from measured data in External Target mode (the Flat Target Auxiliary Data File), thus performing simultaneously the Flat Target Transformation. If the Flat Target Transformation is not used, an artificial constant scene is used, where the visibilities are obtained by multiplying the G-matrix by a constant vector of temperature  $T_{\text{Rec}}$ . For the calculation of the Land and Sea temperatures required for the Gibbs removal, actually only the Land temperature is estimated here, since the sea temperatures vector is determined in the Foreign Sources Module (see Section 2.3.2 for details).

Notice that, like in the current baseline (in the [DPM L1b v2.4](#)), the Visibilities passed on to the L1c processor are in the Fourier space.

---

<sup>5</sup> A Reference Temperature,  $T_{\text{Ref}}$ , is a temperature with respect to which all other temperatures are given, i.e. if  $T_{\text{B}}()$ .

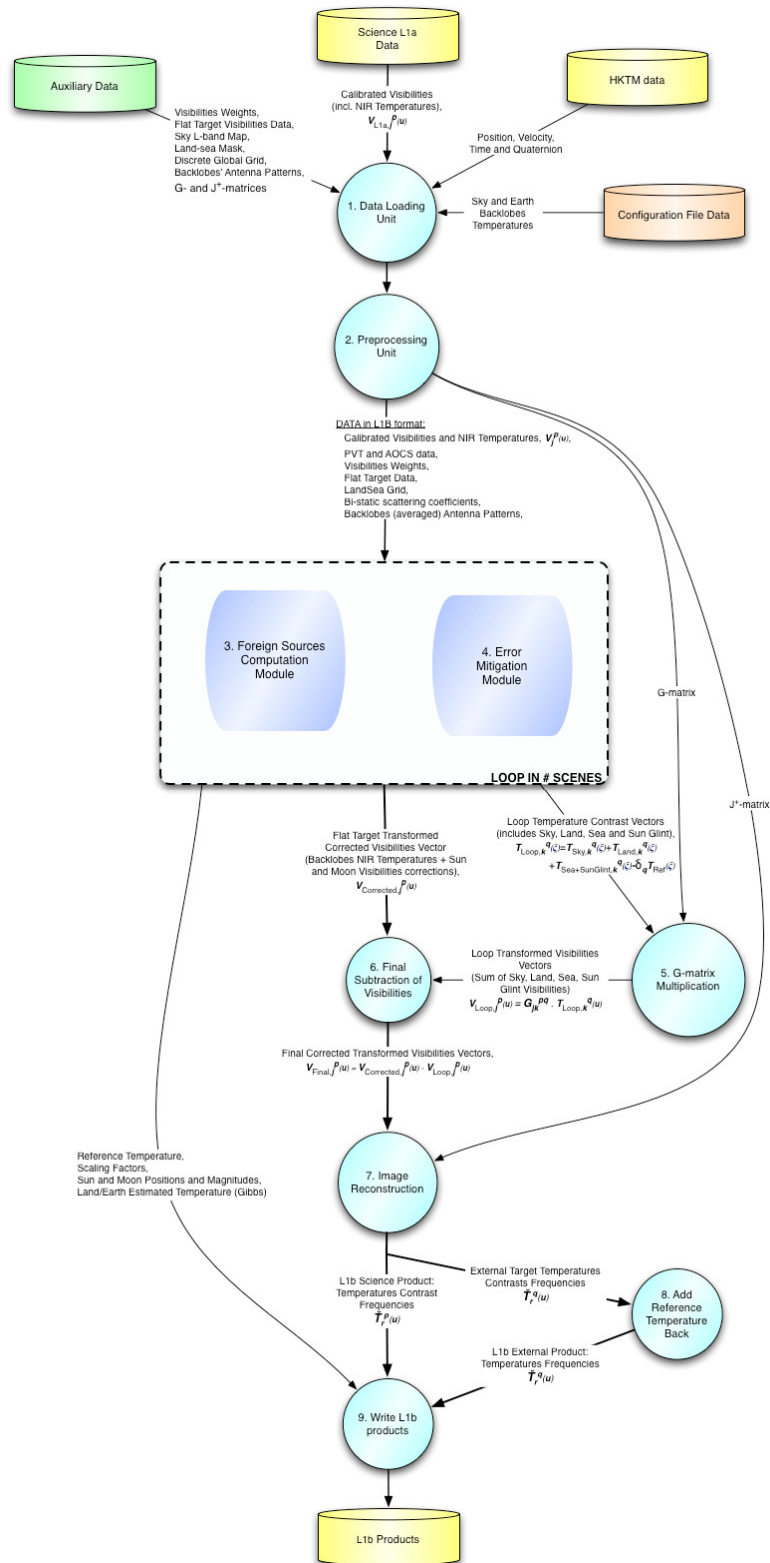


Figure 3: Image Processing Module, including Foreign Sources Correction and Error Mitigation.

### 2.2.1. Zero Baselines Visibilities Processing

A delicate point in the Image Reconstruction is of the processing of the Visibilities corresponding to the zero baselines, or NIR Temperatures. These are special baselines, which are treated differently than the other baselines. The reasons for this distinction are first that NIR Temperatures are absolute temperatures, given with respect to the absolute zero, so there is no Corbella term, whereas for all other baselines the Corbella term is present. The second reason is that some corrections (e.g. backlobes) are only performed for the NIRs. For this reason the processing of the NIR baselines is particularised below in Figure 4. The processing segment shown is very much simplified, since only the path corresponding to the Calibrated Visibilities is shown, and other variables are hidden, but should be obvious where it fits in the global diagram of Figure 3.

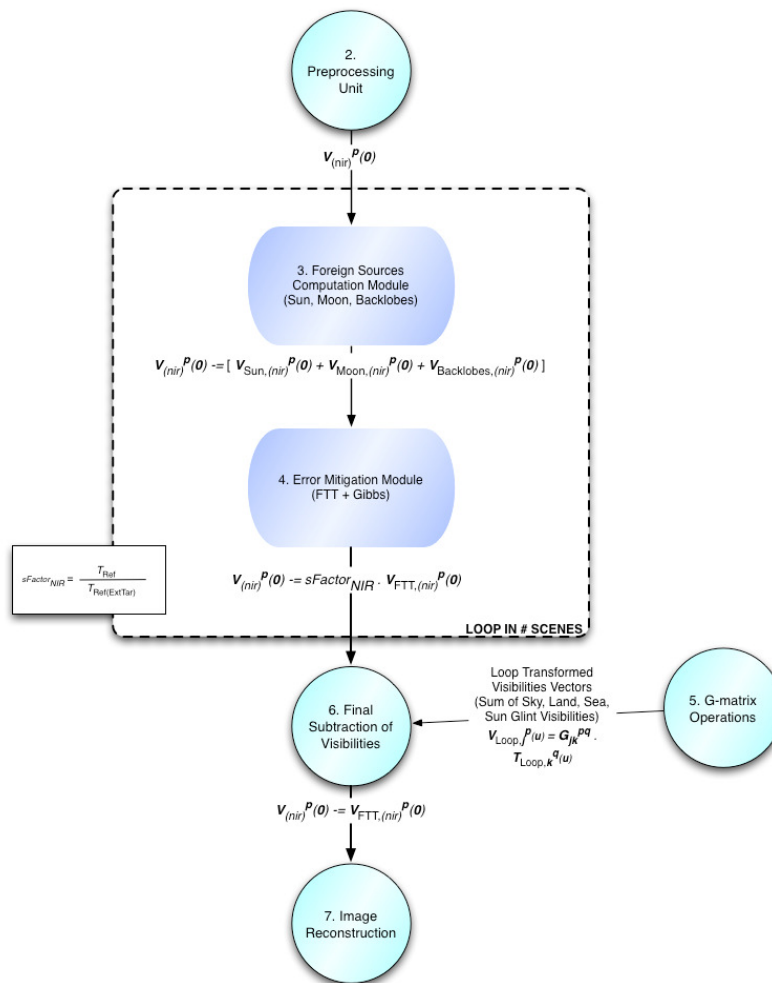
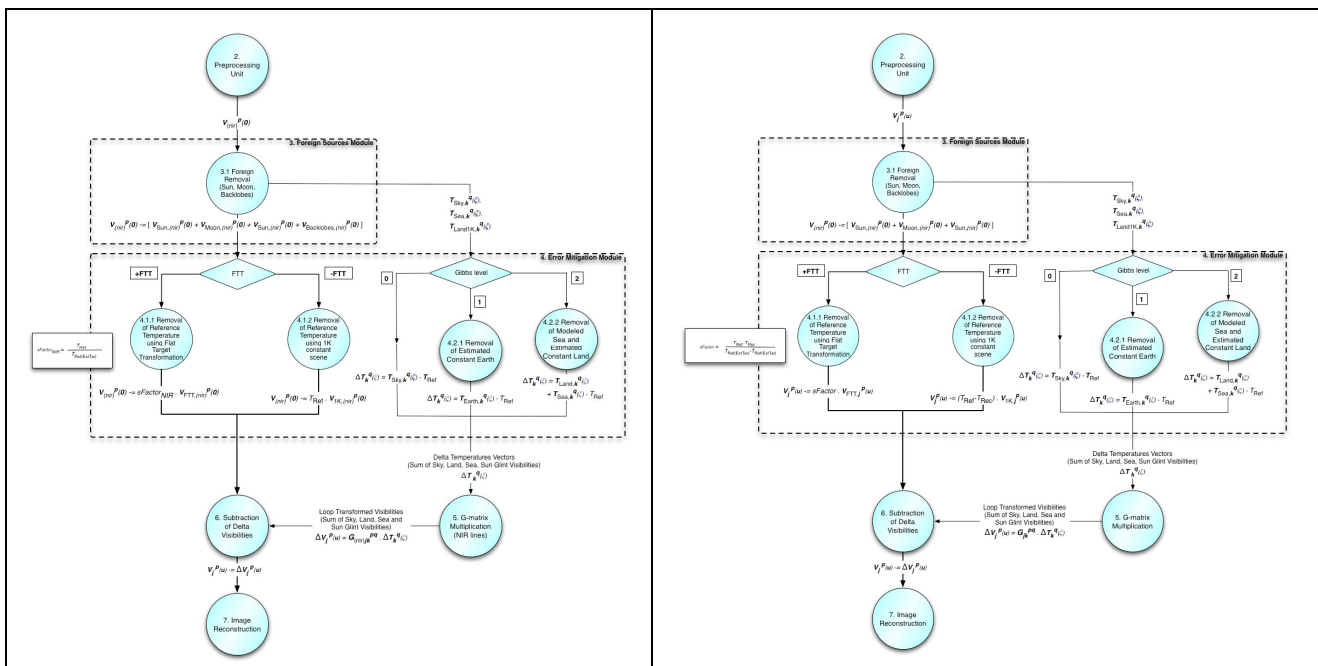


Figure 4: Simplified Data Flow Diagram of the processing of the NIR (zero) baselines.

To allow for a direct comparison of the differences in processing, the Foreign Sources and Error Mitigation Modules were expanded in the next diagrams for the NIR baselines, Figure 5, and for the remaining baselines in Figure 6.

Here it is shown explicitly the transformations that the Calibrated Visibilities go through, namely:

- The Calibrated Visibilities coming from the Preprocessor<sup>6</sup> are fed into the Foreign Sources (FS) module;
- In the FS Module the relevant contributions are calculated and removed. *Notice that the backlobes Visibilities are only corrected for the NIRs.* The Visibilities are then passed on to the Error Mitigation (EM) Module;
- In the EM Module the Reference Temperature is set, either through the Flat Target Transformation (FTT) or the 1K Visibilities. *Notice that the scaling factors for the NIRs is different than for the remaining baselines.* This is because the NIR Temperatures are given wrt the absolute zero in Temperatures, OK, whereas all other baselines are given wrt the Receivers Temperature,  $T_{Rec}$ ;
- In the EM Module the Delta Temperatures needed for the Gibbs removal are also calculated, and sent to the G-matrix Multiplication processing unit to be converted into Visibilities;
- Finally, the Gibbs correction is applied in the Subtraction of Visibilities processing unit, by removing the Delta Visibilities from the Calibrated Visibilities, and the output is then sent to the Reconstruction processing unit.



**Figure 5: Simplified Flowchart of the processing of the zero baselines Visibilities.**

**Figure 6: Simplified Flowchart of the processing of the nominal (i.e. non-zero) baselines Visibilities.**

<sup>6</sup> These are basically the output of the L1a Module, except form format changes. In fact the only difference is that the NIR components in the wrong polarisation are removed, so the Visibilities now fill a vector of size 2346 instead of 2556.

## 2.3. Main Loop

To keep the *Figure 3* from getting too convoluted, the main Loop in the number of scenes was shown as a black box. Its global behaviour is now explained (see *Figure 7*), and it's constituent modules are further detailed in Sections 2.3.1 and 2.3.2.

The main objective of the Main Loop is to compute “delta” visibilities from the measured L1a Calibrated visibilities.

$$V_{LIB}^p(\mathbf{u}) = V_{LIA}^p(\mathbf{u}) - \Delta V^p(\mathbf{u}) \quad \text{Eq. 1}$$

The Delta Visibilities themselves can be summarised as follows:

$$\Delta V_j^p(\mathbf{u}) = \Delta_{FS} V_j^p(\mathbf{u}) + \Delta_{EM} V_j^p(\mathbf{u}) + \Delta' V_j^p(\mathbf{u}) \quad \text{Eq. 2}$$

where:

$\Delta_{FS} V_j^p(\mathbf{u}) = V_{Sun,j}^p(\mathbf{u}) + V_{Moon,j}^p(\mathbf{u}) + V_{Backlobes,j}^p(\mathbf{u})$  are the Delta Visibilities removed in the Foreign Sources Module, consisting of the Direct Sun and Moon, and the Backlobes<sup>7</sup> contributions;

$\Delta_{EM} V_j^p(\mathbf{u}) = V_{Ref,j}^p(\mathbf{u})$  are the Delta Visibilities removed in the Error Mitigation Module, which is simply the removal of the Visibilities corresponding to constant scene at a reference temperature,  $T_{Ref}$ , and includes the Flat Target Transformation;

$\Delta' V_j^p(\mathbf{u}) = V_{Sky,j}^p(\mathbf{u}) + V_{Earth,j}^p(\mathbf{u}) + V_{SunGlint,j}^p(\mathbf{u})$  are the Delta Visibilities which are calculated inside the main loop as Temperatures,  $\Delta T_j^q(\xi)$ . The Temperatures themselves are given by the contributions of a modelled Sky and Earth<sup>8</sup> and the estimated Sun Glint:

$$\Delta T_k^q(\xi) = T_{Sky,k}^q(\xi) + T_{Earth,k}^q(\xi) + T_{SunGlint,k}^q(\xi) - \delta_q T_{Ref}^{-1} \quad \text{Eq. 3}$$

The Delta Visibilities,  $\Delta' V_j^p(\mathbf{u})$ , are obtained from these temperatures through the System Response Function, or G-matrix (see below). Notice that  $\Delta T_j^q(\xi)$  is a Temperature Contrast, since it is given with respect to a Reference Temperature.

### Notation:

In the formulae above and throughout this document, the notation is the following:

$\mathbf{u}$  is a shorthand notation for a  $(u, v)$ -baselines pair;

$\xi$  is a shorthand notation for a  $(\xi, \eta)$  pair;

$\mathbf{j}$  is the  $(u, v)$ -baselines index, also used indiscriminately as the vector index,  $\mathbf{j} \equiv (j_1, j_2)$ , for a pair of antennae;

<sup>7</sup> The Backlobes are corrected only for the NIRs (zero) baselines.

<sup>8</sup> The Earth Temperature being understood as the modelled/estimated Temperature on the Sea and the Land, which should be responsible for the correction of the Gibbs effect near the Earth/Sky border and, in Gibbs Level 2 mode, for the (yet experimental) removal of this effect in the Land/Sea border. See Section 2.3.2 for more details.

$\mathbf{k}$  is the index for the  $(\xi, \eta)$ -grid, and can also be taken as a vector index  $\mathbf{k} \equiv (k_1, k_2)$ ;

$\mathbf{p} \equiv (p_1, p_2)$  is a polarisation vector mode for the pair of antennae  $\mathbf{j} \equiv (j_1, j_2)$  for which the visibilities have been measured;

$\mathbf{q} \equiv (q_1, q_2)$  is the polarisation vector mode of a Temperature scene  $\Delta T_j^q(\xi)$ ;

$\delta_q \equiv \delta_{q_1, q_2}$  is the Kronecker delta, which is one in dual-pol mode, i.e. if  $\mathbf{q} \equiv (\text{H}, \text{H})$  or  $\mathbf{q} \equiv (\text{V}, \text{V})$ , and zero otherwise;

$\mathbf{1}_k$  is a vector of ones.

In order to compute the contribution of the different sources, the system response function should be considered:

$$V_j^p(\mathbf{u}) = \iint_{\xi^2 + \eta^2 \leq 1} \sum_q F_{n, j_1}^{p_1, q_1}(\xi) F_{n, j_1}^{p_2, q_2}(\xi) \frac{T_B^q(\xi)}{\zeta(\xi)} \beta_{\mathbf{k}} e^{-j 2\pi f_0 \Delta t} d\xi d\eta \quad \text{Eq. 4}$$

With

$\zeta(\xi) \equiv \sqrt{1 - \xi^2 - \eta^2}$  the *Obliquity Factor* and

$\Delta t \equiv \frac{u\xi + v\eta + w\zeta(\xi)}{f_0}$  is the *Delay Time*.

This may be redefined in the discrete form as:

$$V_j^p = \sum_{\mathbf{k}} \sum_q F_{n, j_1, \mathbf{k}}^{p_1, q_1} F_{n, j_2, \mathbf{k}}^{p_2, q_2} \frac{T_{B, \mathbf{k}}^q}{\zeta_{\mathbf{k}}} \beta_{\mathbf{k}} e^{-i 2\pi f_0 \Delta t_{j, \mathbf{k}}} dS_{\mathbf{k}} \quad \text{Eq. 5}$$

Where  $\mathbf{u} \rightarrow \mathbf{u}_j$ ,  $\xi \rightarrow \xi_{\mathbf{k}}$ ,  $d\xi d\eta \rightarrow dS_{\mathbf{k}}$  represents the area of each  $(\xi, \eta)$  “pixel” of the integration domain, and the meaning of all other quantities should be obvious.

Finally using matrix notation, the following equation is obtained:

$$V_j = G_{j, \mathbf{k}} T_{\mathbf{k}} \quad \text{Eq. 6}$$

It must be stressed out that the G-Matrix required in Equation 6 must be computed over the complete unit circle, unlike the one used in the Image Reconstruction process, which is only computed in the hexagonal domain (fundamental period).

The grid used in Equation 6 to compute the Brightness Temperature vector distribution,  $T_{\mathbf{k}}$ , is a  $N \times N$  square grid, defined in the  $(\xi, \eta)$  domain  $[-1, 1] \times [-1, 1]$ . In this grid, all the pixels have the same area and the pixels outside the Unit Circle are simply not considered. However, due to the fact that

Eq.5 presents a singularity in the unit circle ( $\zeta_k = 0$ ), the implementation of the square  $(\xi, \eta)$  -grid must “avoid” the unit circle pixels. In order to do so, the  $(\xi, \eta)$  domain should be restricted to the grid pixels that verify the following condition:  $\xi^2 + \eta^2 \leq 0.98$  (instead of considering the domain  $\sqrt{\xi^2 + \eta^2} \leq 1$ ).

In the case of this grid, the  $(\xi, \eta)$  “pixel” area in Eq. 5 is computed as:  $dS_k = dS \equiv \left(\frac{2}{N}\right)^2$ , where  $N \times N$  is the dimension of the grid and N is typically 128.

In order to apply the foreign sources correction algorithm, the Brightness Temperatures of each of the sources identified in Eq.3 shall be determined and the corresponding visibilities computed. The following paragraphs describe the approach followed for determining the Brightness Temperatures of each of the sources.

The Galaxy Map used as baseline contains measurements for HV polarisation, and these shall be used when correcting full pol visibilities. However, there are no sources for Sun or Moon temperatures in HV pol, so they shall be assumed to be zero. New information in this regard may come during commissioning, and never before that.

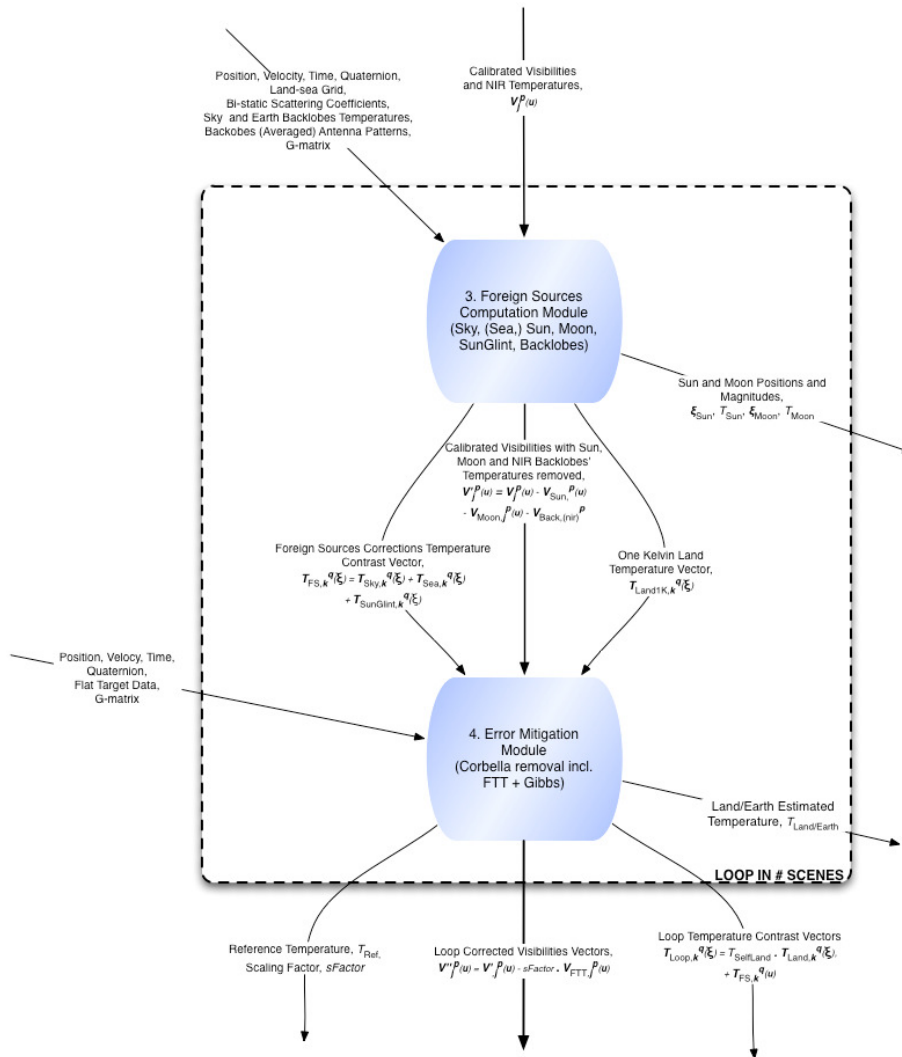


Figure 7: Detailed Data Flow for the loop in the number of scenes.

### 2.3.1. Foreign Sources Computation Sub-module Details

The Foreign Sources Correction Sub-module is needed to remove the influence of external sources in the reconstruction process. This module calculates the Visibilities contributions that are generated by the presence of Sun, Moon or strong Sky. These Visibilities, if properly calculated and subtracted from the calibrated visibilities, should eliminate the strong unwanted sources that appear in the FOV.

For the **Sun removal**, a two-step approach is required, needing as well an initial reconstruction of the uncorrected calibrated visibilities to obtain the Sun truth as measured by MIRAS. The Sun truth is obtained at the nominal and reflected Sun directions (known through S/C position and attitude).

The *direct Sun* contribution may be computed immediately once the Sun temperature is measured in this approach.

For the *Sun Glint* contribution, Sun reflection over the Oceans is modelled through several auxiliary parameters, namely the Sun BT, wind speed and direction, and Sea Surface Salinity and Sea Surface Temperature. This is particularly important on sea reflections, and has some impact as well on land. The surface roughness produces a scattering of the reflected image, lowering the BT at the centre, but affecting a wider area. The current removal strategy consists on the identification of the affected elliptical area, where the Sun energy is distributed. The BT magnitude of the Sun can be obtained from the scene itself.

In any way, any particular correction of each effect is selectable within the module, being possible to activate any, or all of them, if the processing requires it. Information on which correction has been performed shall be part of the L1b product format.

The Foreign Sources Module has the following inputs:

- HKTM L1a Data
- Sky Brightness Temperatures Map
- Default Sun/Moon Brightness Temperatures Maps
- Antenna Patterns (including backlobes)
- System Response Function (G Matrix) previously computed

The effectiveness of these corrections shall be verified during the testing and operations of the L1 Processor prototype. The information on the correction applied and its validity shall be made available to the L2 users within the L1 format. It shall also be possible to generate the L1c data without any correction, such that the L2 users apply any correction they deem required.

The detailed DFD for the Foreign Sources Computation Sub-module is shown in *Figure 8*. It consists of five units:

- 1) Sky Temperatures Calculation: this unit calculates a Sky Temperature Map using the information from the Galaxy L-band ADF and from the PVT and quaternion.
- 2) Sun and Moon Calculation and Removal: Calculates the Sun and Moon Visibilities and removes them from the Calibrated Visibilities, for which requires selected G-matrix columns. The Sun magnitude is estimated here and, together with the Sun position, this information is shared with the next two units.
- 3) Sun Glint Calculation: from the Sun position and magnitude and the bi-static scattering coefficients this unit determines the Sun Glint Temperatures.
- 4) Backlobes Removal: using the average Backlobes' Antenna Patterns, this unit estimates the contribution to the NIR Temperatures, which is due to the backlobes pattern of the antennae. The contribution is removed ONLY for the NIR elements (i.e. zero baseline) and it is performed for both nominal and external target data.
- 5) Earth Calculation: this is a helper unit to the Error Mitigation Module, which uses the Land-sea grid information. It has two possible behaviours, depending on the Gibbs correction level applied:
  - a) For Gibbs 1 correction (removal of constant, estimated Earth) the Sea Temperatures are not removed, and the only action taken is to set the One Kelvin Land Temperatures Vector to one in

the Earth (i.e. Land and Sea). This is passed on to the Error Mitigation Module for the estimation of the Earth constant Temperature;

- b) For Gibbs 2 correction (removal of (constant or not) fixed Sea, and estimated Land), it determines the constant Sea Temperatures Vector, which are added to the previous Temperature corrections above, and a constant One Kelvin Land Temperatures Vector, to be provided to the Error Mitigation Module for Temperature estimation of the Land to be removed.

Notice that the units 1, 3 and 5 above are calculated as Temperature Vectors, and must still be multiplied by the G-matrix in order to be transformed into Visibilities (see Figure 3). The unit 2 corrections (Sun and Moon) are immediately calculated in Visibilities and the correction is immediately applied, and the unit 4 corrections (backlobes) are only applied to the zero baselines (NIRs) and so are also applied here.

Contrary to what happens for the Error Mitigation Sub-module, whose contributions are to be re-added back in the L1c processor, the contributions calculated here are later removed (still in the L1b processor) and are not re-added back. The only exception is the Sea Temperatures in Gibbs 2 correction level, since this must be added back at a later stage.

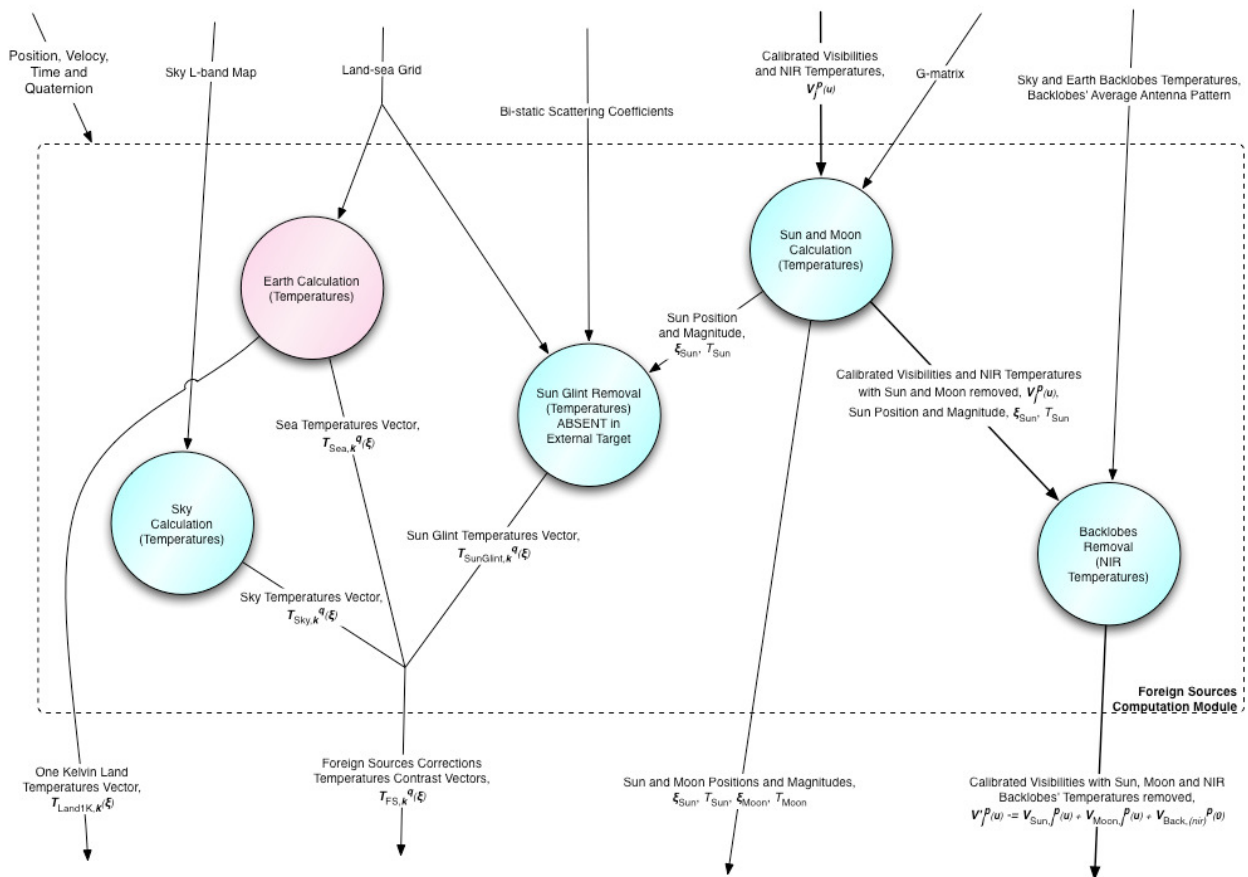


Figure 8: Foreign Sources Calculation Sub-module.

### 2.3.1.1. Compute Sky, Land and Sea pixels

This function is needed to discriminate the NxN unit circle used within Foreign Sources and separate it into Sky and Earth, as well as Land and Sea.

First it is mandatory to initialise the EE-CFI elements used in geolocation, using the same method described in DPM L1c. The function `xp_target_altitude` from the EE-CFI shall be used to determine the Earth-Sky contour. The contour is computed over 6 angular directions then fitted through an ellipse and interpolated to the  $(\xi, \eta)$  grid being used.

The pixels inside the contour are considered Earth, while the remaining ones are considered Sky. As we are using an NxN square grid, the pixels outside the Unit Circle are ignored.

It should be highlighted that when computing the contour of the earth, part of the  $(\xi, \eta)$  pixels corresponding to the contour can actually be on the back of the instrument. For instance, the figure below presents the contour for a tilt angle of 60°:

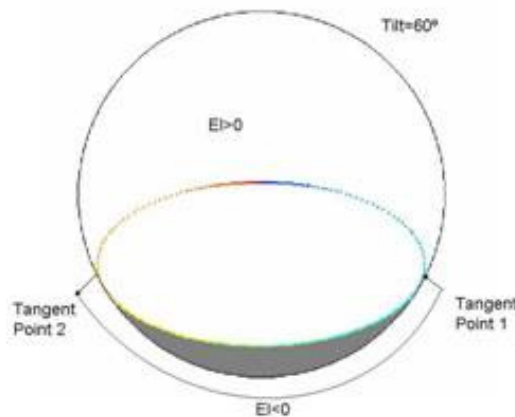


**Figure 9: Contour of the earth computed using the `xp_target_altitude` CFI function**

What is shown in the previous figure is that part of the earth contour ellipse that appears projected in the unit circle belongs to the back of the instrument (segment of the ellipse between “tangent point 1” and “tangent point 2”, with negative elevation). Therefore, for the ellipse pixels that have negative elevation, the contour will appear on the back. That means that, in the previous figure, we will have the following pixels corresponding to the Earth on the front and on the back:

1. Pixels with Earth on the front: grey area + interior of the ellipse;
2. Pixels with Earth on the back: grey area.

This function shall be used to compute which areas of the front and back unit circle belong to Sky or Earth, thus separating the NxN grid into two exclusive pixel lists.

For those pixels within the Earth area of the unit circle, a further decomposition is possible by using the LandSea Mask ADF (`AUX_LSMASK`). This decomposition is performed by transforming each  $(\xi, \eta)$  direction into lat-lon coordinates and using the closest ISEA grid point to retrieve the Landsea mask value.

### **2.3.1.2. Sky Brightness Temperature**

For computing the Sky contribution to the Visibilities, the Brightness Temperatures of the pixels corresponding to the Sky need to be computed.

Using the list of pixels corresponding to the Sky, the right ascension and declination of each of the sky pixel is computed. Since the Galaxy Map ADF contains the temperatures for Right Ascension and

Declination coordinates expressed in B1950 Reference Frame, two transformations are needed before retrieving the galaxy temperatures: Antenna Frame  $\rightarrow$  J2000  $\rightarrow$  B1950. Pseudocode for this transformation can be seen as follows:

```

Compute BF_to_J2000 rotation matrix (identical procedure as L1c DPM section 5.2.4)
For each of the pixels in the sky_xi_eta_list
    Compute BF_vector as [sqrt(1-xi*xi-eta*eta), eta, xi]
    J2000_vector = BF_vector * BF_to_J2000 matrix
    dec=asin(J2000_vector[2]);ra=atan2(J2000_vector[1], J2000_vector[0]);

    Apply Kraus '63 equations to correct ra_J2000 and dec_J2000 values due to
    precession and nutation changes from J2000 origin to snapshot time
    m_2000 = 3.07420
    n_2000_time = 1.33589
    n_2000_arc = 20.0383
    m_now = 3.07420 + 0.0000186*time
    n_now_time = 1.33589 - 0.0000057* time
    n_now_arc = 20.0383 - 0.000085* time
    /*correct ra and dec for precession effects from current time to galaxy map epoch
    J2000 */
    ra_change_2000 = (m_2000 + n_2000_time*sin(ra)*tan(dec))*time
    dec_change_2000 = (n_2000_arc*cos(ra))*time
    ra_change_now = (m_now + n_now_time*sin(ra + ra_change_2000/86636.5554*2*PI)*
    tan(dec + dec_change_2000/1296000*2*PI))*time
    dec_change_now = (n_now_arc*cos(ra + ra_change_2000/86636.5554*2*PI))*time
    ra_2000 = (ra + 0.5*(ra_change_2000 + ra_change_now)/86636.5554*2*PI)
    dec_2000 = (dec + 0.5*(dec_change_2000 + dec_change_now)/1296000*2*PI)

    Convert(Right Ascension, Declination) in J2000 to (Right Ascension, Declination)
    in B1950
    R[0] = cos(ra_2000)*cos(dec_2000)
    R[1] = sin(ra_2000)*cos(dec_2000)
    R[2] = sin(dec_2000)
    A[0][0] = 0.9999256791774783;   A[0][1] = 0.0111815116959975;   A[0][2] =
    0.0048590037714450
    A[1][0] = -0.0111815116768724;   A[1][1] = 0.9999374845751042;   A[1][2] = -
    0.0000271704492210
    A[2][0] = -0.0048590038154553;   A[2][1] = -0.0000271625775175;   A[2][2] =
    0.9999881946023742
    ra_1950 = atan2((A*R)[1], (A*R)[0])
    dec_1950 = asin((A*R)[2])

    Get Galaxy Temperatures From ADF using (Right Ascension, Declination) in B1950
End

```

Finally, using Right Ascension and Declination, the Brightness Temperatures of those pixels are determined with the help of the L-Band Galaxy Map ADF which contains the maps of the galactic emission at 1420 MHz (SM\_XXXX\_AUX\_GLXY\_<ID>).

The resulting Temperatures, obtained directly from the L-Band Galaxy Map ADF, which contains the maps of the galactic emission at 1420 MHz (SM\_XXXX\_AUX\_GLXY\_<ID>), are expressed as Stokes Parameters, and they need to be converted to brightness temperatures.

If the polarisation axes of the Galaxy Map and the MIRAS instrument were aligned, the conversion would be the following one:

$$\begin{aligned}
 T_H &= \frac{I+Q}{2} \\
 T_V &= \frac{I-Q}{2} \\
 T_{HV} &= \frac{Q}{2} + \frac{U}{2}i
 \end{aligned}
 \tag{Eq. 7}$$

As the polarisation frame of the Galaxy Map and the polarisation frame of the instrument are not aligned, a further rotation is needed before computing the Brightness Temperatures in the MIRAS polarisation frame. At the time of closing this document, this rotation angle is TBD.

### 2.3.1.3. Earth Brightness Temperature

The new Gibbs removal method is based on the algorithm used prior to this baseline. Its purpose is to remove spatial gradients from the image before reconstruction and to add them back in Brightness Temperatures instead of Frequencies to avoid contamination from the Gibbs ripples.

There shall be two methods for doing this. The first one will remove only the Earth-Sky gradient, by computing a constant Earth value for all pixels in the unit circle that correspond to the Earth. The second method will go further and remove also the Land-Sea contour by using a constant Sea or a Sea model for Sea pixels and estimate a constant Land for Land pixels.

In the end, the visibilities are computed, as for the other sources, taking into account the system response function:

$$V_{Earth}^{pq}(u, v) = G(u, v; \xi, \eta) T_{Earth}^{pq}(\xi, \eta)
 \tag{Eq. 8}$$

The equation used to estimate the constant Earth or Land Brightness Temperature is given by the following expression, as described in [RD.11], such that the mean brightness temperature value of the scene to be imaged is zero:

$$T_{Land}^{pq} = \frac{T_A^{pq} - V_{Sky+Sea+Sun/Moon+Sun\ glint+Back}^{pq}(0, 0)}{\bar{V}_{Land}^{pq}(0, 0)}
 \tag{Eq. 9}$$

Where  $\bar{V}_{Land}^{pq} = G(u, v; \xi, \eta) T_{Land\ 1K}^{pq}(\xi, \eta)$  are the visibilities that would be measured considering the Earth or Land areas in the unit circle as a uniform source with BT=1Kelvin and the term  $T_A^{pq}$  is the antenna temperature at a given polarisation, which for horizontal and vertical polarisation can be computed from the instrument output (NIR) and for cross-polarisation contribution it is computed from the self-correlations between LICEF\_NIR in H and V ports.

As can be immediately observed, the only difference in the two methods lies in which area of the unit circle is going to be used for the constant Brightness Temperature estimation. For the first method, the whole Earth is considered to be estimate and no Sea Brightness Temperature will be computed. For the second method, only the Land part will be used in the estimation, assuming that the Brightness Temperature distribution of the Sea part is constant or known through the model.

#### 2.3.1.4. Sea Brightness Temperature model

The Brightness Temperatures over Sea are computed according to:

$$T_v(\theta) = (1 - \Gamma_v(SST, SSS, \theta))SST + 0.2 \left(1 - \frac{\theta}{55^\circ}\right) WS$$

$$T_h(\theta) = (1 - \Gamma_h(SST, SSS, \theta))SST + 0.2 \left(1 + \frac{\theta}{55^\circ}\right) WS$$

**Eq. 10**

Where:

SST – is the Sea Surface Temperature, assumed to be 15°C;

SSS – is the Sea Surface Salinity, assumed to be 35psu;

WS – is the Wind Speed, assumed to be 4m/s;

$\theta$  – is the elevation angle from pixel to S/C

The Fresnel reflections coefficients model that has been used is the Klein&Swift '77 for sea water.

#### 2.3.1.5. Direct Sun and Moon Visibilities

This algorithm will both compute and correct the effect of the Sun/Moon point sources in the L1a Calibrated Visibilities.

First of all, the Sun/Moon positions in the antenna frame need to be computed using the Earth Explorer CFI libraries (*xl\_sun* and *xl\_moon*) and the instrument attitude. Since both Sun and Moon are seen from MIRAS as point sources, their contribution will be limited to a single pixel in the  $(\xi, \eta)$  domain<sup>9</sup>.

After determining the body  $(\xi, \eta)$  position in the antenna frame, the Sun/Moon Brightness Temperatures is computed. One of the three following approaches can be used for determining the Sun/Moon Temperatures:

1. Estimate from the L1A visibilities (only applicable to the Sun);
2. Read from an Auxiliary Data File if measurements are available (SM\_XXXX\_AUX\_SUNT\_<ID> / SM\_XXXX\_AUX\_MOONT\_<ID>);
3. Use default values - 110.000K for the SUN H and V Temperature; 250K for the Moon H and V Temperatures. For HV polarisation the default values of the temperatures are currently set to 0, and will only be updated if a suitable default value is found during the commissioning phase.

<sup>9</sup> Since the sun and moon are seen as point sources, the corresponding visibilities will be computed using the exact  $(\xi, \eta)$  positions of the bodies instead of using the pre-defined  $(\xi, \eta)$  square/polar grids (described in section **Error! Reference source not found.**) which may introduce important approximation errors on the positions of the sources.

Once the Brightness Temperatures of the Sun/Moon are computed, the corresponding visibilities may be obtained from the following equation [RD.12, Equation 17]:

$$V_{Sun/Moon,dir}^{pq}(u,v) = T_{Sun/Moon,dir}^{pq} \cdot \bar{V}_{Sun/Moon,dir}^{pq}(u,v) \quad \text{Eq. 11}$$

where:

$T_{Sun/Moon,dir}^{pq}$  - is the Sun/Moon temperature (estimated from visibilities, read from an ADF or using default values);

$\bar{V}_{Sun/Moon,dir}^{pq}(u,v)$  - corresponds to the visibility samples (without units) that would be measured by the instrument corresponding to unitary point sources located at the positions of the direct sun/moon.

The following paragraphs explain how to compute the terms  $T_{Sun/Moon,dir}^{pq}$  and  $\bar{V}_{Sun/Moon,dir}^{pq}(u,v)$ .

### 2.3.1.5.1. Estimation of the Sun Brightness Temperature from the Visibilities - $T_{Sun,dir}^{pq}$

The estimation of the Sun/Moon brightness temperatures from the visibilities may be performed following the approach described in [RD.12], i.e., if we consider negligible fringe-washing effects,  $\tilde{r}_{j,k} = 1$ , and similar antenna patterns, i.e.  $F_{n,j}(\xi_k) = F_n(\xi_k)$ , Eq.5 reduces to something similar to a Discrete Fourier Transform<sup>10</sup> :

$$V_j^q = \sum_k |F_n(\xi_k)|^2 \frac{T_B^p(\xi_k) - T_{Rec} \delta_p}{\zeta(\xi_k)} e^{-i2\pi\Delta t/f_0} dS_k \quad \text{Eq. 12}$$

$$\Leftrightarrow V_j^q = DFT^{-1}(T_B^p(\xi_k))$$

where

$$T_{Mod}^p(\xi_k) \equiv \sum_k |F_n(\xi_k)|^2 \frac{T_B^p(\xi_k) - T_{Rec} \delta_p}{\zeta(\xi_k)} dS_k \quad \text{Eq. 13}$$

is a modified Brightness Temperature used in the computation,  $F_n(\xi_k)$  corresponds to the average of the 72 existing antenna patterns measurements and  $dS_k = \sqrt{3}d^2/2$  corresponds to the pixel area in the  $(u,v)$  domain (as described in [RD.13]).

The terms  $\bar{V}_{Sun,dir}^{pq}$  can then be estimated from the visibilities as described in [RD.16, Equations 1 to 4]:

<sup>10</sup> Eq.12 is not the exact definition of a DFT but could be re-defined as such by using a mathematical manipulation of the exponential term (see for instance Eq. 23 of [RD.13] showing a similar Inverse DFT case).

$$T_{Sun,dir}^{pq} = \frac{T_{Raw}^{pq}}{\bar{T}_{Sun,dir}^{pq}} = \frac{F^{-1}(V^{pq}(u,v) - V_{Rec}^{pq}(u,v))}{F^{-1}(\bar{V}_{Sun,dir}^{pq}(u,v))} \quad \text{Eq. 14}$$

Where:

$V^{pq}(u,v)$  - corresponds to the calibrated L1a visibilities;

$T_{Raw}^{pq}$  - is a “raw” brightness temperature image;

$\bar{T}_{Sun,dir}^{pq}$  - is the instrument’s response for a 1 K amplitude point-source computed in the direction of the pixel corresponding to the Sun direction;

$V_{Rec}^{pq}(u,v)$  - Receivers visibilities, as described in DPM L1b v2.4, Section 3.3.1.5.

$\bar{V}_{Sun/Moon,dir}^{pq}(u,v)$  - corresponds to the visibility samples (without units) that would be measured by the instrument corresponding to unitary point sources located at the positions of the direct sun;

Although not documented in [RD.16], UPC proposed an additional improvement on the sun estimation algorithm, which allowed obtaining the results presented in [RD.17]. This modification consists on the usage of some knowledge of the scene brightness temperature for improving the estimation in Eq. 14, by modifying its numerator:

$$T_{Sun,dir}^{pq} = \frac{T_{Raw}^{pq}(\xi_{Sun}, \eta_{Sun}) - T_{Scene Average}^{pq}}{\bar{T}_{Sun,dir}^{pq}(\xi_{Sun}, \eta_{Sun})} = \frac{F^{-1}(V^{pq}(u,v) - V_{Rec}^{pq}(u,v)) - T_{Scene Average}^{pq}}{F^{-1}(\bar{V}_{Sun,dir}^{pq}(u,v))} \quad \text{Eq. 15}$$

Where  $T_{Scene Average}^{pq}$  is computed as the average of the raw image -  $T_{Raw}^{pq}$  - in the vicinity of the Sun position  $(\xi_{Sun}, \eta_{Sun})$ . After several simulations, UPC concluded that the best results are obtained when  $T_{Scene Average}^{pq}$  is computed as the average over a  $[11 \times 11]$  pixels square, centred at the Sun position -  $(\xi_{Sun}, \eta_{Sun})$ .

According to [RD.16], although it has to be confirmed from radio-astronomical measurements, one can assume that for cross polarisation,  $T_{Sun,dir}^{HV} = 0$ .

#### Implementation details:

The Inverse Fourier Transforms presented in are implemented using standard rectangular FFT libraries. However, as explained previously, the FFT routines cannot be applied directly to the hexagonal visibilities samples.

In order to apply rectangular FFTs, the visibilities need to be re-arranged in a  $[N \times N]$  rectangular matrix. This visibilities re-arrangement process, detailed below, is also described in [AD.12], section 6.35:

1. first we compute the rectangular  $[N \times N]$  sampling grid as explained in Eq. 4 of the DPM L1b v2.4 document and Eqs. 22a of [RD.13]:

$$(u_{FFT}, v_{FFT}) = \left( \frac{d}{2}(k_1 + 2k_2), \frac{\sqrt{3}d}{2}k_1 \right), \text{ where } k_1, k_2 \in [0; N-1];$$

2. then, for each visibility sample  $V(u, v)$ , we will check which is the position  $(k_1, k_2)$  on the sampling grid that verifies the condition:

$$\left| (u_{FFT}(k_1, k_2), v_{FFT}(k_1, k_2)) - (u, v) \right| < \frac{d}{4};$$

3. Finally, we add to the  $(k_1, k_2)$  position of a  $[N \times N]$  Visibilities matrix (initially padded with zeros), the visibility samples  $V(u, v)$  divided by the  $(u, v)$  pair redundancy:

$$V_{FFT}(k_1, k_2) = V_{FFT}(k_1, k_2) + \frac{V(u, v)}{N(u, v)}$$

where  $N(u, v)$  is the total number of visibility samples corresponding to the frequency  $(u, v)$ .

After the application of the previous steps for re-arranging the visibilities, the FFT routines can be used. It should be highlighted that the  $T(\xi, \eta)$  matrixes obtained as output of the FFT will be sorted according to the  $(\xi_{FFT}, \eta_{FFT})$  grid defined by Eq. 4 of the DPM L1b v2.4:

$$(\xi_{FFT}, \eta_{FFT}) = \left( \frac{1}{N_T d} k_1, \frac{1}{\sqrt{3} N_T d} (k_1 + 2k_2) \right).$$

It should be highlighted that the algorithm described in this section for the Sun BT estimation from the visibilities, although could theoretically be applied both to the Sun and to the Moon, only performs well for the Sun estimation. The conclusions reached by UPC (and implemented in SEPS) are that the technique does not work directly for the Moon, due to the fact that  $T_{Moon,dir}^{pq} \ll T_{Sun,dir}^{pq}$  and  $T_{Moon,dir}^{pq}$  is of the order of magnitude of  $T_{Earth}^{pq}$ , being the moon confused with the Earth background. Therefore the estimate of the moon brightness temperature is set to a fixed value of 250 K.

Finally it should be remarked that the Sun brightness temperatures estimation is only performed when the Sun appears in the front of the instrument. When it appears on the back, due to the fact that the backlobe antenna patterns are 30dB lower than the boresight, the effect of the Sun perturbation will be very low, which means that the corresponding brightness temperatures can not be estimated accurately.

### 2.3.1.5.2. Computation of the Sun/Moon visibilities corresponding to a 1K source -

$$\bar{V}_{Sun/Moon,dir}^{pq}$$

The term  $\bar{V}_{Sun/Moon,dir}^{pq}(u, v)$  from Eq.11 can be computed using the System response function. i.e.:

$$\bar{V}_{\text{Sun/Moon,dir};j}^p(\mathbf{u}) = \iint_{\xi^2 + \eta^2 \leq 1} \sum_q \frac{F_{n,j_1}^{p_1,q_1}(\xi) F_{n,j_1}^{p_2,q_2}(\xi)}{\sqrt{\Omega_1 \Omega_2}} \frac{1}{\zeta(\xi)} h(\xi - \Delta t) e^{-j2\pi f_0 \Delta t} d\xi d\eta \quad \text{Eq. 16}$$

However, as described in [RD.16], a singularity problem arises when one tries to compute  $V_{\text{Sun,dir}}^{pq}(u, v)$  when the Sun position is close to the unite circle ( $\xi^2 + \eta^2 = 1$ ), that is, when the Sun is 90° away from the boresight direction. If the Sun is considered as a point source, this problem is overcome by changing the coordinate system from the  $(\xi, \eta)$  director cosines to the spherical one:

$$\begin{aligned} \xi &= \sin \theta \cos \phi \\ \eta &= \sin \theta \sin \phi \end{aligned} \quad \text{Eq. 17}$$

Eq. 16 will then become:

$$V_{\text{Sun,dir}}^{pq} = \frac{1}{\sqrt{\Omega_1 \Omega_2}} \int_0^{2\pi} \int_0^\pi T_{B,\text{Sun}}(\theta, \phi) F_{n,1}^p(\theta, \phi) F_{n,2}^{q*}(\theta, \phi) \tilde{r}_{12} \left( -\frac{u_{12} \sin \theta \cos \phi + v_{12} \sin \theta \sin \phi + w_{12} \cos \theta}{f_0} \right) \exp(-j2\pi(u_{12} \sin \theta \cos \phi + v_{12} \sin \theta \sin \phi + w_{12} \cos \theta) \sin \theta) d\theta d\phi \quad \text{Eq. 18}$$

where, for a point source Sun, we have:

$$T_{B,\text{Sun}}(\theta, \phi) = \frac{T_{B,\text{Sun}0} \Omega_{\text{Sun}}}{\sin \theta_{\text{Sun}}} \delta(\theta - \theta_{\text{Sun}}) \delta(\phi - \phi_{\text{Sun}}) \quad \text{Eq. 19}$$

According to [RD.16], when trying to account for the Sun's finite beamwidth, the integration of Eq. 18 becomes more difficult and an additional coordinate transformation is needed. Accounting as well for the Cross-polar Antenna Patterns, the visibilities corresponding to the Sun ( $V_{\text{Sun,dir}}^{pq}$ ) can be expressed as follows:

$$\begin{aligned}
 V_{Sun,dir}^{xx} &= \frac{1}{\sqrt{\Omega_1 \Omega_2}} \iint_{\xi^2 + \eta^2 \leq 1} \frac{(R_{x,1} R_{x,2}^* + C_{x,1} C_{x,2}^*) T_{B,Sun.}(\xi, \eta)}{\sqrt{1 - \xi^2 - \eta^2}} \tilde{r}_{12} \left( -\frac{u_{12} \xi + v_{12} \eta + w_{12} \sqrt{1 - \xi^2 - \eta^2}}{f_0} \right) e^{-j2\pi(u_{12} \xi + v_{12} \eta + w_{12} \sqrt{1 - \xi^2 - \eta^2})} d\xi d\eta = \\
 &= \frac{\Omega_{Sun}}{\sqrt{\Omega_1 \Omega_2}} T_{B,Sun.}(\theta_{Sun}, \phi_{Sun}) [R_{x,1} R_{x,2}^* + C_{x,1} C_{x,2}^*] \tilde{r}_{12} \left( -\frac{u_{12} \sin \theta_{Sun} \cos \phi_{Sun} + v_{12} \sin \theta_{Sun} \sin \phi_{Sun} + w_{12} \cos \phi_{Sun}}{f_0} \right) \\
 &\quad \exp(-j2\pi(u_{12} \sin \theta_{Sun} \cos \phi_{Sun} + v_{12} \sin \theta_{Sun} \sin \phi_{Sun} + w_{12} \cos \phi_{Sun})) \\
 &\quad \left\{ 1 + \left[ j \frac{w_{12}''}{2} - \frac{1}{12\pi} - \frac{\pi}{2} (u_{12}'' + v_{12}'') \right] \Omega_{Sun} \right\}
 \end{aligned} \tag{Eq. 20}$$

$$\begin{aligned}
 V_{Sun,dir}^{yy} &= \frac{1}{\sqrt{\Omega_1 \Omega_2}} \iint_{\xi^2 + \eta^2 \leq 1} \frac{(R_{y,1} R_{y,2}^* + C_{y,1} C_{y,2}^*) T_{B,Sun.}(\xi, \eta)}{\sqrt{1 - \xi^2 - \eta^2}} \tilde{r}_{12} \left( -\frac{u_{12} \xi + v_{12} \eta + w_{12} \sqrt{1 - \xi^2 - \eta^2}}{f_0} \right) e^{-j2\pi(u_{12} \xi + v_{12} \eta + w_{12} \sqrt{1 - \xi^2 - \eta^2})} d\xi d\eta = \\
 &= \frac{\Omega_{Sun}}{\sqrt{\Omega_1 \Omega_2}} T_{B,Sun.}(\theta_{Sun}, \phi_{Sun}) [R_{y,1} R_{y,2}^* + C_{y,1} C_{y,2}^*] \tilde{r}_{12} \left( -\frac{u_{12} \sin \theta_{Sun} \cos \phi_{Sun} + v_{12} \sin \theta_{Sun} \sin \phi_{Sun} + w_{12} \cos \phi_{Sun}}{f_0} \right) \\
 &\quad \exp(-j2\pi(u_{12} \sin \theta_{Sun} \cos \phi_{Sun} + v_{12} \sin \theta_{Sun} \sin \phi_{Sun} + w_{12} \cos \phi_{Sun})) \\
 &\quad \left\{ 1 + \left[ j \frac{w_{12}''}{2} - \frac{1}{12\pi} - \frac{\pi}{2} (u_{12}'' + v_{12}'') \right] \Omega_{Sun} \right\}
 \end{aligned} \tag{Eq. 21}$$

and

$$\begin{aligned}
 V_{Sun,dir}^{yx} &= \frac{1}{\sqrt{\Omega_1 \Omega_2}} \iint_{\xi^2 + \eta^2 \leq 1} \frac{(C_{y,1} R_{x,2}^* + R_{y,1} C_{x,2}^*) T_{B,Sun.}(\xi, \eta)}{\sqrt{1 - \xi^2 - \eta^2}} \tilde{r}_{12} \left( -\frac{u_{12} \xi + v_{12} \eta + w_{12} \sqrt{1 - \xi^2 - \eta^2}}{f_0} \right) e^{-j2\pi(u_{12} \xi + v_{12} \eta + w_{12} \sqrt{1 - \xi^2 - \eta^2})} d\xi d\eta = \\
 &= \frac{\Omega_{Sun}}{\sqrt{\Omega_1 \Omega_2}} T_{B,Sun.}(\theta_{Sun}, \phi_{Sun}) [C_{y,1} R_{x,2}^* + R_{y,1} C_{x,2}^*] \tilde{r}_{12} \left( -\frac{u_{12} \sin \theta_{Sun} \cos \phi_{Sun} + v_{12} \sin \theta_{Sun} \sin \phi_{Sun} + w_{12} \cos \phi_{Sun}}{f_0} \right) \\
 &\quad \exp(-j2\pi(u_{12} \sin \theta_{Sun} \cos \phi_{Sun} + v_{12} \sin \theta_{Sun} \sin \phi_{Sun} + w_{12} \cos \phi_{Sun})) \\
 &\quad \left\{ 1 + \left[ j \frac{w_{12}''}{2} - \frac{1}{12\pi} - \frac{\pi}{2} (u_{12}'' + v_{12}'') \right] \Omega_{Sun} \right\}
 \end{aligned} \tag{Eq. 22}$$

where

- $R_{pn}$  and  $C_{pn}$  are respectively the co- and cross-polar antenna patterns at p-polarization corresponding to the nth antenna;
- $\Omega_{Sun}$  is the sun solid angle which is:  $\Omega_{Sun} = \frac{\pi}{4} \beta_{sun}^2 = \frac{\pi}{4} (0.586)^2$ ;

-  $\begin{bmatrix} x'' \\ y'' \\ z'' \end{bmatrix} = \begin{bmatrix} \cos \theta_{Sun} & 0 & -\sin \theta_{Sun} \\ 0 & 1 & 0 \\ \sin \theta_{Sun} & 0 & \cos \theta_{Sun} \end{bmatrix} \cdot \begin{bmatrix} \cos \phi_{Sun} & \sin \phi_{Sun} & 0 \\ -\sin \phi_{Sun} & \cos \phi_{Sun} & 0 \\ 0 & 0 & 1 \end{bmatrix} \cdot \begin{bmatrix} x \\ y \\ z \end{bmatrix}$  and the baselines, defined in  $(x, y, z)$  coordinate system  $(u_{12}, v_{12}, w_{12}) = (x_2 - x_1, y_2 - y_1, z_2 - z_1) / \lambda$  become:

$$\begin{cases} u_{12}'' = \cos \theta_{Sun} \cos \phi_{Sun} u_{12} + \cos \theta_{Sun} \sin \phi_{Sun} v_{12} - \sin \theta_{Sun} w_{12} \\ v_{12}'' = -\sin \phi_{Sun} u_{12} + \cos \phi_{Sun} v_{12} \\ w_{12}'' = \sin \theta_{Sun} \cos \phi_{Sun} u_{12} + \sin \theta_{Sun} \sin \phi_{Sun} v_{12} + \cos \theta_{Sun} w_{12} \end{cases} \quad \text{Eq.23}$$

**Implementation details:** As described in Section 3.1 of the DPM L1b v2.4, the selection of a particular  $(\xi - \eta)$  indexes in the G-Matrix system response function corresponds to selecting a particular column of the matrix. However, from an implementation point of view, the term  $\bar{V}_{Sun/Moon,dir}^{pq}$  cannot be computed from the System response function due to the following factors:

1. the G-Matrix function is computed for a fixed  $(\xi, \eta)$  grid while the Sun/Moon appear at precise  $(\xi_{S/M}, \eta_{S/M})$  positions that need to be used with accuracy (grid approximation errors need to be avoided for these point sources);
2. The “pixel area” used in the G-Matrix computation -  $d\xi d\eta = \left(\frac{2}{N}\right)^2$  - is different from the Sun/Moon point sources area;
3. The Obliquity Factor, which caused the singularity close to the unit circle, disappears from the Equations 32 to 34 of the DPM L1b v2.4 due to the usage of a different coordinate system.

On the other hand, computing “manually” equations 32 to 34 of the DPM L1b v2.4, implies, from an implementation/architecture point of view, loading the 72 antenna patterns Auxiliary Files and the Fringe Washing Function product before computing the  $\bar{V}_{Sun/Moon,dir}^{pq}$  term.

Therefore, in order to minimise the impact on the architecture as well as the computational overhead, the approach proposed for computing  $\bar{V}_{Sun/Moon,dir}^{pq}$  is based on the usage of the G-Matrix (which is already loaded when processing the Foreign Sources Correction) and applying different correction factors.

Recalling the System Response Function, defined previously we have:

$$G(u, v; \xi, \eta) = \frac{1}{\sqrt{1 - \xi^2 - \eta^2}} \frac{\hat{F}_k(\xi, \eta) \hat{F}_j^*(\xi, \eta)}{\sqrt{\Omega_k \Omega_j}} \hat{r}_{kj} \left( -\frac{u\xi + v\eta + wOF}{f_0} \right) e^{-j2\pi(u\xi + v\eta + wOF)} d\xi d\eta$$

By particularising the  $(\xi - \eta)$  indexes for the points in the G-Matrix spatial grid closer to the Sun/Moon positions -  $(\xi_{S/M \text{ grid}}, \eta_{S/M \text{ grid}})$  - we get the G-Matrix columns corresponding respectively to the co-polar

and cross-polar contributions to the visibilities of a point source located at  $(\xi_{S/M \text{ grid}}, \eta_{S/M \text{ grid}})$ :  $G_R(u, v; \xi_{S/M \text{ grid}}, \eta_{S/M \text{ grid}})$  and  $G_C(u, v; \xi_{S/M \text{ grid}}, \eta_{S/M \text{ grid}})$ .

If we consider that the fringe washing function and the antenna patterns do not present high variations, we may assume that:

$$\frac{\hat{F}_k(\xi_{S/M \text{ grid}}, \eta_{S/M \text{ grid}}) \hat{F}_j^*(\xi_{S/M \text{ grid}}, \eta_{S/M \text{ grid}})}{\sqrt{\Omega_k \Omega_j}} \hat{r}_{kj} \left( -\frac{u \xi_{S/M \text{ grid}} + v \eta_{S/M \text{ grid}} + w OF_{S/M \text{ grid}}}{f_0} \right) \approx \frac{\hat{F}_k(\xi_{S/M}, \eta_{S/M}) \hat{F}_j^*(\xi_{S/M}, \eta_{S/M})}{\sqrt{\Omega_k \Omega_j}} \hat{r}_{kj} \left( -\frac{u \xi_{S/M} + v \eta_{S/M} + w OF_{S/M}}{f_0} \right)$$

Where  $(\xi_{S/M}, \eta_{S/M})$  and  $(\xi_{S/M \text{ grid}}, \eta_{S/M \text{ grid}})$  correspond respectively to the exact Sun/Moon position and to the spatial sample on the G-Matrix grid closer to the real Sun/Moon position.

Rewriting Equations 32 and 33 of the DPM L1b v2.4, taking into account the previous considerations, we have:

$$\begin{aligned} \bar{V}_{Sun,dir}^{pp} &= \frac{[R_{p,1} R_{p,2}^* + C_{p,1} C_{p,2}^*]}{\sqrt{\Omega_1 \Omega_2}} \tilde{r}_{12} \left( -\frac{u_{12} \xi_{S/M} + v_{12} \eta_{S/M} + w_{12} \sqrt{1 - \xi_{S/M}^2 - \eta_{S/M}^2}}{f_0} \right) \\ &= e^{-j2\pi(u_{12} \xi_{S/M} + v_{12} \eta_{S/M} + w_{12} \sqrt{1 - \xi_{S/M}^2 - \eta_{S/M}^2})} \cdot \Omega_{S/M} \cdot \left\{ 1 + \left[ j \frac{w_{12}''}{2} - \frac{1}{12\pi} - \frac{\pi}{2} (u_{12}'' + v_{12}'') \right] \Omega_{S/M} \right\} = \\ &= (G_R(u, v; \xi_{S/M \text{ grid}}, \eta_{S/M \text{ grid}}) + G_C(u, v; \xi_{S/M \text{ grid}}, \eta_{S/M \text{ grid}})) \cdot F_{OF} \cdot F_{exp} \cdot F_{pixel \text{ area}} \end{aligned}$$

Where  $F_{OF}$ ,  $F_{exp}$  and  $F_{pixel \text{ area}}$  are the correction factors applied to the G-Matrix in order to obtain  $\bar{V}_{Sun/Moon,dir}^{pq}$ :

$$F_{OF} = \sqrt{1 - \xi_{S/M \text{ grid}}^2 - \eta_{S/M \text{ grid}}^2} \text{ - factor for correcting the division by the OF performed in the G-Matrix computation;}$$

$$F_{exp} = \frac{e^{-j2\pi(u_{12} \xi_{S/M} + v_{12} \eta_{S/M} + w_{12} \sqrt{1 - \xi_{S/M}^2 - \eta_{S/M}^2})}}{e^{-j2\pi(u_{12} \xi_{S/M \text{ grid}} + v_{12} \eta_{S/M \text{ grid}} + w_{12} \sqrt{1 - \xi_{S/M \text{ grid}}^2 - \eta_{S/M \text{ grid}}^2})}} \text{ - factor used for correcting the Sun/Moon position error introduced by the exponential term in the G-Matrix, when approaching the Sun/Moon position using the grid;}$$

$$F_{pixel\ area} = \frac{\Omega_{S/M} \cdot \left\{ 1 + \left[ j \frac{w_{12}''}{2} - \frac{1}{12\pi} - \frac{\pi}{2} \left( (u_{12}'')^2 + (v_{12}'')^2 \right) \right] \Omega_{S/M} \right\}}{\left( \frac{2}{N} \right)^2} - \text{factor for correcting the pixel area}$$

introduced in the G-Matrix and for adding the area factor corresponding to the new coordinate system and to the fact that the Sun/Moon are seen as finite disks.

Following this approach, one can compute the  $\bar{V}_{Sun/Moon,dir}^{pq}$  simply using the G-Matrix and a priori knowledge of the Sun/Moon position.

### 2.3.1.6. Sun Glint Brightness Temperature

For the Sun glint, Sun reflection over Oceans shall be modelled through several auxiliary parameters, namely the Sun BT, the incidence and scattered angles of each pixel with respect to the sun and some pre-computed scattering coefficients.

The Sun Glint Effect removal is based on an algorithm proposed by N. Reul from IFREMER. According to this algorithm (see Annex of the DPM L1b v2.4), the solar energy scattered by a given surface impinging the antenna at the position  $(\xi, \eta)$  in the director cosine frame is represented by the radiometric temperature:

$$T_{Bsun\ glint}^H(\xi, \eta) = \frac{1}{4\pi \cos \theta} \int_0^{2\pi} \int_0^{\beta_{sun}/2} \left[ \sigma_{HH}^0(\bar{n}_s, \bar{n}_i) + \sigma_{HV}^0(\bar{n}_s, \bar{n}_i) \right] T_{Sun}(\bar{n}_i, t) d\Omega_i \quad \text{Eq. 24}$$

$$T_{Bsun\ glint}^V(\xi, \eta) = \frac{1}{4\pi \cos \theta} \int_0^{2\pi} \int_0^{\beta_{sun}/2} \left[ \sigma_{VV}^0(\bar{n}_s, \bar{n}_i) + \sigma_{VH}^0(\bar{n}_s, \bar{n}_i) \right] T_{Sun}(\bar{n}_i, t) d\Omega_i \quad \text{Eq. 25}$$

Where:

$\sigma_{HH}^0, \sigma_{VV}^0, \sigma_{HV}^0, \sigma_{VH}^0$  – are the bistatic scattering coefficients of the sea surface for HH, VV, HV and VH polarisations respectively;

$\bar{n}_i = \bar{n}_i(\theta, \phi)$  – is the direction (incidence and azimuth angles) of Sun radiations at the earth surface position  $(\varphi, \psi)$  corresponding to the MIRAS coordinates  $(\xi, \eta)$  at time t;

$\bar{n}_s = \bar{n}_s(\theta_s, \phi_s)$  – is the direction (incidence and azimuth angles) of the scattered Sun glint signals;

$\theta$  – is the scattering elevation angle<sup>11</sup>;

$\beta_{sun}/2 \approx 0.02931/4$  – is the angular radius of the Sun as viewed from the Earth;

$T_{Sun}(\vec{n}_i, t)$  – is the brightness temperature of the Sun at 1.4GHz in the direction  $\vec{n}_i$  and time  $t$ .

Equations 24 and 25 can be further simplified by considering that within the solid angle subtended by the Sun as seen from any of the observed terrestrial targets, the local Sun direction  $\vec{n}_i$  is almost constant:

$$T_{Bsun\ glint}^{pq}(\xi, \eta, t) = \frac{T_{Sun}(\vec{n}_i, t) \Omega_{sun}}{4\pi \cos \theta} \left[ \sigma_{pp}^0(\vec{n}_s, \vec{n}_i) + \sigma_{pq}^0(\vec{n}_s, \vec{n}_i) \right] \quad \text{Eq. 26}$$

where  $\Omega_{sun}$  (steradian) is the solid angle intercepting the Sun as seen from the earth:

$$\Omega_{sun} = 2\pi \left[ 1 - \cos\left(\frac{\beta_{sun}}{2}\right) \right] \cong 8.2 \times 10^{-5} [sr] \quad \text{Eq. 27}$$

In order to determine the bistatic scattering coefficients the following sea surface parameters at the target  $T = (\varphi, \psi, t)$  need to be known:

- The sea surface salinity (SSS);
- The sea surface temperature (SST);
- The 10 meter height wind speed and direction ( $U_{10}, \varphi_u$ ).

As demonstrated in [RD.11], the effect of the Sun BT is dominant in the modelling of the Sun glint, and using averaged values for the other variables does not introduce relevant errors. These averaged values are SSS = 35 [psu], SST = 15 [°C],  $U_{10} = 10 [m/s]$ ,  $\varphi_u = \text{TBD}$ . Usage of this model is considered as the baseline for computing the Reflected Sun contribution to be subtracted to the visibilities.

Previous studies show that due to the small sensitivity of the computed Sun glint temperature  $T_{Bsun\ glint}^{pq}(\xi, \eta, t)$  to the variations of SSS, SST and wind speed and direction, one can assume the following globally averaged mean values: SSS = 35 [psu], SST = 15 [°C],  $U_{10} = 10 [m/s]$ ,  $\varphi_u = \text{TBD}$ .

The approach proposed by N. Reul is to determine the bistatic scattering coefficients from Look-Up-Tables (LUT) based on the following parameters:

- Sun incidence angle –  $\theta_i$  [deg];

<sup>11</sup> Since the incidence and scattering elevation angles may be different (depending on the pixel),  $\theta$  is computed as the average between incident and scattered angle:  $\theta = \frac{\theta_i + \theta_s}{2}$ .

- ❑ Relative azimuth angle between Sun and MIRAS observation angle –  $\phi_i - \phi_s$  [deg];
- ❑ MIRAS observation incidence angle –  $\theta_s$  [deg];
- ❑ The 10 meter height wind speed and direction  $(U_{10}, \phi_u)$ .
- ❑ The LUT currently being used contains information only for  $U_{10} = 7 [m/s]$ .
- ❑ This algorithm receives as input the Sun Brightness Temperature computed in Section 2.3.1.1 and the pixels corresponding to the Earth and determines, for the  $(\xi, \eta)$  pixels corresponding to the ocean the following parameters:
  - ❑ Sun (to pixel) incidence direction –  $(\theta_i, \phi_i)$ ;
  - ❑ Pixel to MIRAS observation angles –  $(\theta_s, \phi_s)$ ;
  - ❑ These parameters, computed using EE CFI Pointing library allow to compute the three parameters needed for retrieving the scattering coefficients:  $\theta_i, \phi_i - \phi_s, \theta_s$ . These three parameters are used to interpolate the LUT and obtain the scattering coefficients for each of the pixels.
  - ❑ Finally applying Eq. 26,  $T_{B_{Sun\ glint}}^{pq}(\xi, \eta)$  is computed for each  $(\xi, \eta)$  corresponding to the ocean and passed to the Sun Glint BT vector. The  $(\xi, \eta)$  positions of the vector that do not correspond to the ocean are set to zero.

### 2.3.1.7. Backlobes Visibilities

The Brightness Temperature distribution entering through the backlobes has an effect that is highly dependent on the level of the backlobes radiating patterns (which are very low). As it has been shown during the IVT campaigns that the level of these backlobes pattern is very close to the noise level with which they were measured, the measurements themselves are not very reliable.

It is then assumed that the Backlobe correction performed in L1b will only be a first order correction over the NIR baselines.

In order to compute the Backlobes visibilities an Auxiliary Data File, which represents the average of the 72 antennas patterns for the backlobes shall be used. As we only compute the NIR baselines, there are no fringe-washing effects ( $\tilde{r}_{kj}(i, j, k, l) = 1$ ) and the backlobes visibilities can be computed using an equation similar to Eq.12:

$$V_{Back}^{pq}(0,0) = \sum_i \sum_j \left| \overline{F}_{Back}(\xi_{i,j}, \eta_{i,j}) \right|^2 \frac{T_{Back}^{pq}(\xi_{i,j}, \eta_{i,j})}{OF(\xi_{i,j}, \eta_{i,j})} dS_{i,j} \quad \text{Eq. 28}$$

Where:

$$T_{Back}^{pq}(\xi, \eta) = T_{Sun/Moon\ dir}^{pq}(\xi_{S/M}, \eta_{S/M}) + T_{Sky}^{pq}(\xi_{Sky}, \eta_{Sky}) + T_{Earth}^{pq}(\xi_{Earth}, \eta_{Earth}) \quad \text{Eq. 29}$$

represents the addition of the different sources that appear on the back of the instrument.

In order to compute Eq. 29, the pixels corresponding to the Earth and Sky in the back of the instrument are determined. For these pixels,  $T_{Sky}^{pq}$  and  $T_{Earth}^{pq}$  are set to default values: 2.7K and 290K respectively<sup>12</sup>.

The term  $T_{Sun/Moon\ dir}^{pq}$  is only used if the Sun/Moon appear on the back of the instrument (otherwise it is set to zero). However, as described in Section 2.3.1.1 the Sun/Moon brightness temperatures are not estimated when the Sun/Moon appear on the back. Therefore, for the pixels corresponding to the Sun/Moon,  $T_{Sun/Moon\ dir}^{pq}$  shall be set to the latest estimation of the Sun/Moon temperatures. If no estimation was performed previously, default values read from Auxiliary Data Files shall be used.

### 2.3.2. Error Mitigation Sub-module

In Figure 10 the DFD for the detailed Error Mitigation sub-module is shown. It consists of two smaller independent units:

- 1) Removal of Flat Target Visibilities: here the Flat Target Visibilities,  $V_{Sky,j}(\mathbf{u})$ , (obtained by the instrument while in External Target Mode) are loaded from the FTT ADF and subtracted from incoming Calibrated Visibilities ( $V'_j(\mathbf{u}) = V_j(\mathbf{u}) - V_{Sky,j}(\mathbf{u})$ ). The Flat Target Scaling Factor,  $sFactor$ , is also calculated and passed on to the L1c.
- 2) Gibbs Calculation: this unit is responsible for estimating the Land Temperature,  $T_{Land}$ , corresponding to the list of pixels that belong to the Earth or Land area in the unit circle (depending on the Gibbs level applied). The output is then a Temperatures Vector,  $T_{Land}+T_{Sea}$ , with values  $T_{Land}$  for the pixels that fall on land and  $T_{Sea}$  on the sea pixels. This unit was absent in the LIPP v1.5 and previous versions. The estimated Land Temperature,  $T_{Land}$ , is also passed on to the L1c processor such that the constant land can be re-added there. Notice that, contrary to what happens in the Flat Target unit above, the Land and Sea contribution is not removed from the Calibrated Visibilities at this point, but only at a later stage (see *Figure 3*).

---

<sup>12</sup> Taking into account the fact that the backlobes contribution is very small, it was preferred to use default values for the Earth and Sky contribution instead of computing the exact Sky BT for each pixel. This allows having a better algorithm performance without penalising in a significant way the precision of the Backlobes BT computation.

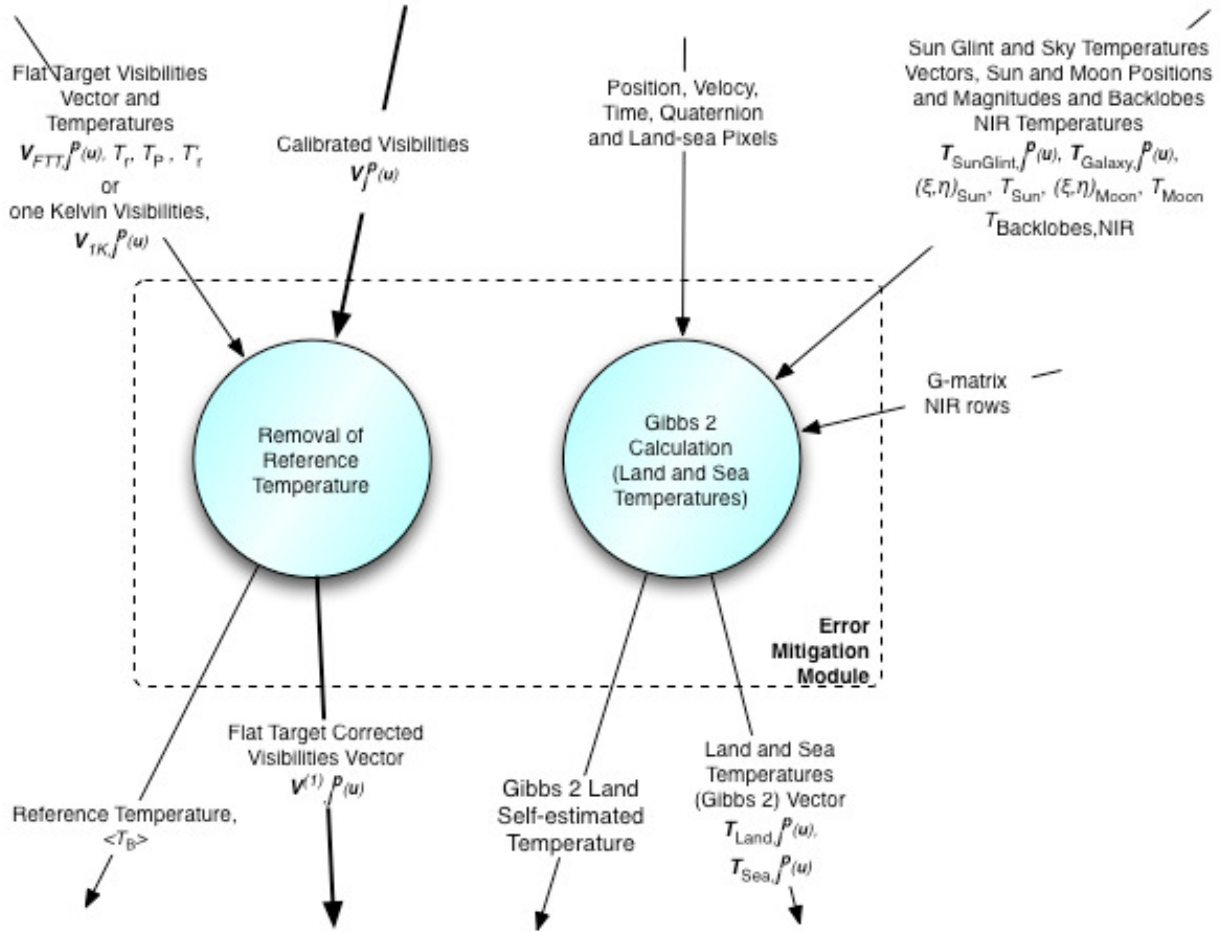


Figure 10: Error Mitigation sub-module.

### 2.3.2.1. Removal of the Reference Temperature Contribution and the Flat Target Transformation

The first step in the Error Mitigation module is to set a global Reference Temperature for the Visibilities. This is especially important since the NIR (zero) baselines are given as absolute temperatures, i.e. with respect to the absolute zero, but all other baselines are given with respect to the receivers temperature,  $T_{Rec}$ . The general form of this correction term is

$$\begin{aligned}
 \Delta V_{EM,(nir)}^q(\mathbf{0}) &= \delta_q T_{Ref} V_{1K,(nir)}^q(\mathbf{0}), \text{ for the NIR} \\
 \Delta V_{EM,j}^q(\mathbf{u}) &= \delta_q (T_{Ref} - T_{Rec}) V_{1K,j}^q(\mathbf{u}), \text{ for the all other baselines}
 \end{aligned}
 \tag{Eq.30}$$

If no Flat Target is used, the LIPP determines the 1K Visibilities by multiplying a 1K vector by the G-matrix, however, the default algorithm is to perform simultaneously a Flat Target Transformation to reduce the errors in the antenna patterns. In this case the term that sets the Reference Temperature to  $T_{Ref}$  is:

$$\Delta V_{EM,(nir)}^q(\mathbf{0}) = \delta_q \frac{T_{Ref}}{T'_{Ref}} V_{FTT,(nir)}^q(\mathbf{0}), \text{ for the NIR}$$

$$\Delta V_{EM,j}^q(\mathbf{u}) = \delta_q \frac{T_{Ref} - T_{Rec}}{T'_{Ref} - T'_{Rec}} V_{FTT,j}^q(\mathbf{u}), \text{ for the all other baselines}$$

**Eq. 31**

where:

$V_{FTT,j}(\mathbf{u})$  is the measurement of a set of FTT calibrated visibilities, obtained while the instrument is pointing to the deep sky;

$T_{Ref}$  is the Reference Temperature<sup>13</sup>;

$T_{Rec}$  is the average of the physical temperature of the receivers for the scene being observed;

$T'_{Ref}$  is the Brightness Temperature of the zone being observed during the acquisition of  $V_{FTT,j}^q(\mathbf{u}; T'_{Ref} - T'_{Rec})$ ;

$T'_{Rec}$  is the average of the physical temperature of the receivers during the acquisition of  $V_{FTT,j}^q(\mathbf{u}; T'_{Ref} - T'_{Rec})$ ;

The equation above is valid for all baselines except for the NIR units, which are not affected by the Corbella term. For these NIR units, a similar scaling factor shall be applied, but without using the  $T_{Rec}$  or  $T'_{Rec}$  values.

It shall be remarked that this correction has the effect of changing the offset of the Brightness Temperature scene that shall be reconstructed to  $T_{Rec}$ . This means, that a correction to the final BT Fourier components is required, by simply adding this averaged term to the L1b output. As opposed to the previous implementation of the FTT, no further corrections are required to the Brightness Temperature output (e.g. no adding back of FTT Sky or 1K visibilities).

It is important to highlight that the physical temperatures of the receivers are not applicable to HV polarisation, so the corresponding correction term is zero in full polarisation mode, for all baselines.

## 2.4. L1c Implications

In Figure 11 the DFD for the restructured L1c, including the changes induced by the L1b restructuring, is shown. The fact that in the L1PP v1.6 the Gibbs correction is now applied, for Gibbs level 2, in the Land and Sea separately, implies that it has to be re-added back in L1c using the same LandSea mask, so that the borderlines coincide in the two steps (removal and re-addition).

<sup>13</sup> The choice of the Reference Temperature used in the L1PP is configurable by a “Reference Temperature flag”. The allowed possibilities are 0, for zero Kelvin,  $T_{Ref} = 0$ ; 1, for the average of the NIR temperatures in each pol,

$T_{Ref}^p = \delta_p \delta_{pq} \langle V_{NIR}^q \rangle$ ; 2, for the average of the NIR Temperatures in both polarisations  $T_{Ref} = \frac{\langle V_{NIR}^H + V_{NIR}^V \rangle}{2}$ . The default is the last option, the average in both polarisations.

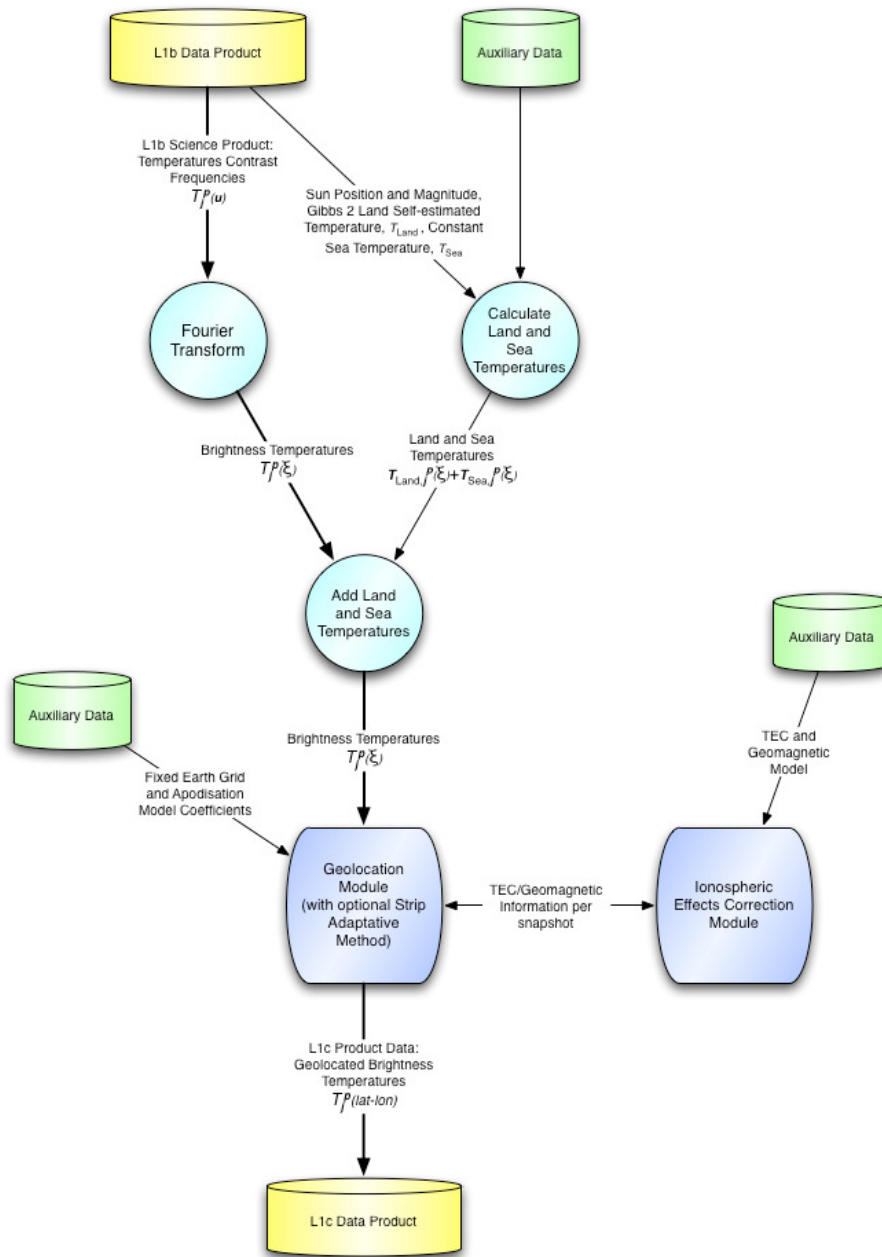


Figure 11: L1c DFD

### 3. MEMORY MANAGEMENT DESIGN OPTIONS

The main algorithm design decision to be taken is whether to optimise the new L1b algorithms for speed and flexibility or for a more universal platform support. In practice, the choice is between loading large amounts of data (G- and J<sup>+</sup>-matrices) in the initial processing sub-units of the L1b Module or to load the matrices in blocks in order not to exceed the available system memory.

The approach followed in the current LIPP implementation, v1.5, was to lower the memory requirements of the machine by loading, whenever necessary, the biggest amounts of data (i.e. the G-matrix) in blocks. However, this involves a more convoluted design and is therefore less flexible and more prone to software problems and mistakes. Also, since the cross-pol terms of the dual parts of both the G and J<sup>+</sup>-matrices will be discarded, the memory requirements for the Image Reconstruction have decreased: in Full-pol, for example, to load a complete G-matrix "only" ~4.4GiB<sup>14</sup> are needed, instead of the ~8GiB needed until now. Finally, since the Ideal Reconstruction mode will still be available in the new L1b, even in Full-pol, it will be possible to process any kind of data in most machines, as the memory requirements of the Ideal Reconstruction mode are much lower.

Due to the above, in the new L1b design the approach is to use the smallest data structures necessary and to load all data at the start of the processing module and to keep the processing routines as straightforward and flexible as possible.

In the case of Dual-pol, for example, two matrix blocks of 4695x128<sup>2</sup> are loaded, one for H-pol and another for V-pol, which amounts to a total of ~1.1GiB (see Table 3). Adding to this the size of a J<sup>+</sup>-matrix (two blocks of 2791x4695) and the size of two Calibrated Visibilities vectors (2x4695) for each polarisation (x2) and for each scene in a product (x2500) and a Temperatures vector also for each polarisation for each scene (2500x2x2791) gives a total of ~2.3GiB of memory needed (see Table 3). For Full-pol the memory requirements rise to ~7.0GiB, so the LIPP should run comfortably still on an 8GiB dedicated machine.

Quantity	Type	Size in Dual-pol mode	Size in Full-pol mode
G-matrix	double	2 x 4695 x 1282 x 8B ≈ 1.15GiB	1.15GiB + 6606 x 4 x 1282 x 8B ≈ 4.37GiB
J+-matrix	double	2 x 2791 x 4695 x 8B ≈ 200MiB	200MiB + 5582 x 15996 x 8B ≈ 881MiB
Visibilities for a half-orbit (2x)	double	2 x 2500 x 2 x 4695 x 8B ≈ 358MiB	2 x 2500 x 15996 x 8B ≈ 610MiB
Temperatures for a half-orbit	double	2500 x 2 x 1282 x 8B ≈ 625MiB	2500 x 4 x 1282 x 8B ≈ 1.22GiB
TOTAL:		~2.3GiB	~7.0GiB

**Table 3: Memory footprint for the largest data structures needed in L1b.**

<sup>14</sup> The binary storage units prefixes used here are according to the IEC standard (see [http://en.wikipedia.org/wiki/Binary\\_prefix#IEC\\_standard\\_prefixes](http://en.wikipedia.org/wiki/Binary_prefix#IEC_standard_prefixes)).



## 4. L1B FLAGS

In the L1PP, the optional behaviour is selected through processing flags. In the Table 4 below the L1b processing flags and their function are summarised for both Nominal (Science) and External Target processing. The entries in **bold** mean that the flag is new, and was not present in the L1PP before v1.6:

Flag	Type	Science Data Behaviour	External Target Behaviour
sun_direct	bool	Applies direct Sun removal	
moon_direct	bool	Applies direct Moon removal	
earth_background	float	Temperature used for Earth removal in the background	
sky_background (was galactic_background)	float	Temperature for Sky removal in the background	
sun_glint (was sun_reflected)	bool	Applies Sun Glint correction	(no effect)
backlobes	bool	Applies backlobes NIR contributions removal	
flat_target_transformation	bool	Applies Flat Target Transformation	
<b>Reference Temperature Level</b>	int	0. Reference Temperature set to 0K 1. Reference Temperature set to average of NIR Temperature for each polarization (a different reference temperatures for each polarization) 2. Reference Temperature set to the average of the NIR Temperatures in both polarizations (same reference temperature for both polarizations)	
<b>use_ftt_reference_temp</b>	bool	Sets Reference Temperature to $\langle T_B \rangle$ (instead of 0)	
sky_direct (was galaxy_direct)	bool	Applies Sky removal	(no effect)

Flag	Type	Science Data Behaviour	External Target Behaviour
sky_direct_external	bool	(no effect)	Applies Sky removal
gibbs_level <sup>15</sup>	int	0. Gibbs removal not performed. 1. Removal of constant, <b>estimated Earth</b> (Land and Sea) Temperature; 2. Removal of <b>modelled (Fresnel), fixed Sea</b> Temperature and <b>constant estimated Land</b> Temperature; 3. Removal of <b>constant, fixed Sea</b> Temperature and constant <b>estimated Land</b> Temperature ( <b>not implemented</b> ); 4. Removal of constant Sky Temperature, <b>measured Land and Sea</b> Temperatures ( <b>future implementation</b> ).	

Table 4: L1b processing flags.

<sup>15</sup> Add this info to the products.

## 5. BREAKPOINTS AND LOGS

Table 5 shows, in the third column, the breakpoint names implemented in the Image Reconstruction Module of the new L1b (in L1PP v1.6). Where applicable, the corresponding breakpoint names in the old L1PP version (prior to v1.6) are also show in brackets. The first column indicates the location in the L1PP implementation where the breakpoint is taken (see the diagram of *Figure 3*), and the common prefix in the breakpoints filenames.

Location (Prefix)	Description	Breakpoint Name	Format
After INPUT DATA (11b_ir_input)	L1a Calibrated Visibilities	visibs_<snapshot_id>_<pol>.txt (was 11b_calibvis_Dual_<p1>_<p1>+<p2>.txt)	2556 x 2 float [ real imag ]
	Baseline Weights	weights_<pol>.txt	4695 x 1 float
	Average Backlobes Antenna Patterns	patt99.txt (was 11b_ap_amplitude_99.txt and 11b_ap_phase_99.txt)	16384 x 14 float [k1 k2 xi eta re(F <sup>X</sup> ) im(F <sup>X</sup> ) re(F <sup>Y</sup> ) im(F <sup>Y</sup> ) re(X <sup>X</sup> ) im(F <sup>X</sup> ) re(X <sup>Y</sup> ) im(X <sup>Y</sup> )]
	G-matrix NIR rows	gMatrixNIR.txt	2*16384 x 2 float [ NIR-AB ] [ NIR-BC ] [ NIR-CA ] (alternate columns for H and V)
	Visibilities for a constant 1K scene	visibs1K_<pol>.txt	4695 x 1 float
After PREPROCESSOR (11b_ir_prepr)	Xi, Eta in the Hexagon (Dual & Full)	xiEta_hexagon.txt	16384 x 2 float [xi eta]
	(u,v)-baselines and Apodisation Window	baselines_apodisationWindow.txt	1396 x 3 [ u v apodWin ]
	Flat Target Product Visibilities	visibs_fft.txt (was 11b_FttVisibsRead.txt)	4695 x 2

	Flat Target Product Temperatures	temp_fit.txt (was 11b_FttTempsRead.txt)	1 x 1
	L1b Calibrated Visibilities	visibs_<snapshot_id>_<pol>.txt	4695 x 1
	Xi, Eta in the Unit Circle	xiEta_unitCircle.txt	16384 x 2 [ xi eta ]
In FOREIGN SOURCES MODULE <sup>16</sup> (11b_fs)	Backlobes Brightness Temperatures	backlobes_tempsSpace_<snapshot_id>_<pol>.txt	16384 x 1
	Sky Brightness Temperatures in the Hexagon	sky_tempsSpace_<snapshot_id>_<pol>.txt	16384 x 1
	1K Land Brightness Temperatures in the Hexago	land1K_tempsSpace_<snapshot_id>_<pol>.txt	16384 x 1
	Sea Brightness Temperatures in the Hexagon	sea_tempsSpace_<snapshot_id>_<pol>.txt	16384 x 1
After FS (11b_ir_frSrc)	Calibrated Visibilities with Sun, Moon and NIR backlobes removed	visibs_<snapshot_id>_<pol>.txt	4695 x 1
After EM (11b_ir_erMtg)	Delta Temperatures	tempsSpace_<snapshot_id>_<pol>.txt	16384 x 1
	Delta Visibilities	visibs_<snapshot_id>_<pol>.txt	4695 x 1
After RECONSTR. (11b_ir_recon)	Temperatures in Frequency space (Dual & Full)	tempsFreqs_<snapshot_id>_<pol>.txt (was 11b_temp_<snapshot_id>_<pol#>.txt)	2791 x 1
	Temperatures in (xi,eta)-space (IFT of tempsFreqs) (Dual & Full)	tempsSpaceIft_<snapshot_id>_<pol>.txt (was 11b_ifft_<snapshot_id>_<pol#>.txt)	16384 x 1

<sup>16</sup> In the LIPP v1.6, for the Foreign Sources breakpoints of the <type> ‘land1K\_tempsSpace’, ‘sea\_tempsSpace’ and ‘sunGlint\_temp’, the Dual-pol breakpoint name corresponding to mixed scenes are given the <pol> superscript ‘F’, instead of the correct one, ‘H’ or ‘V’, and the Full-pol scenes are labelled 11b\_fs\_<type>\_full\_<snapshot\_id>\_F.txt, instead of 11b\_fs\_<type>\_<snapshot\_id>\_F.txt (the SPR 399 was raised with this issue).

**Table 5: L1b breakpoints and validation status.**

## 6. INTERNAL NOTES

From the Progress Meeting #1 (L1PP Phase 4):

- MMN suggests using the following condition to produce external target measurements:
  - o Only produce flat target data when the sun on the back doesn't fall on the sky alias
  - o No correction for the Sun in the back should be done on the generation of the flat target products
  - o This should impact only the planning, i.e., it is assumed that the External Target data received by L1PP already respects the constraints mentioned
- Conclusion of the discussion:
  - o How do we produce flat target? Pure FT or applying corrections? Conclusion: don't apply corrections but make sure that a flat scene is used (0.1K RMS) and only correct NIRs backlobes; Product will contain more information than necessary (which is not used).
- MMN mentions that the description of the FTT in the DPM L1b should be detailed. In particular, the removal of the physical temperature during the FTT generation should be explicitly described.